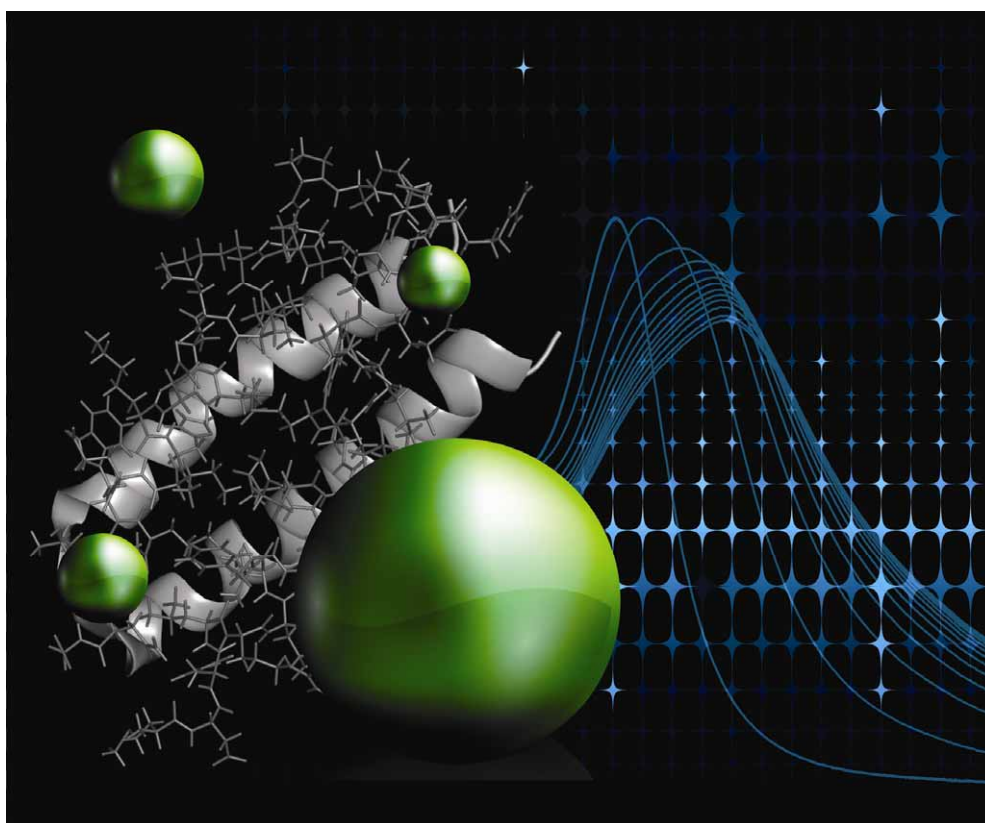


Chem Soc Rev

This article was published as part of the
Peptide- and protein-based materials
themed issue

Guest editors Rein Ulijn and Dek Woolfson

Please take a look at the issue 9 2010 [table of contents](#) to
access other reviews in this themed issue



Molecular self-assembly and applications of designer peptide amphiphiles†

Xiubo Zhao,^{ab} Fang Pan,^a Hai Xu,^{ab} Mohammed Yaseen,^a Honghong Shan,^b Charlotte A. E. Hauser,^c Shuguang Zhang^{cd} and Jian R. Lu^{ab}

Received 7th January 2010

DOI: 10.1039/b915923c

Short synthetic peptide amphiphiles have recently been explored as effective nanobiomaterials in applications ranging from controlled gene and drug release, skin care, nanofabrication, biomineralization, membrane protein stabilization to 3D cell culture and tissue engineering. This range of applications is heavily linked to their unique nanostructures, remarkable simplicity and biocompatibility. Some peptide amphiphiles also possess antimicrobial activities whilst remaining benign to mammalian cells. These attractive features are inherently related to their selective affinity to different membrane interfaces, high capacity for interfacial adsorption, nanostructuring and spontaneous formation of nano-assemblies. Apart from sizes, the primary sequences of short peptides are very diverse as they can be either biomimetic or *de novo* designed. Thus, their self-assembling mechanistic processes and the nanostructures also vary enormously. This *critical review* highlights recent advances in studying peptide amphiphiles, focusing on the formation of different nanostructures and their applications in diverse fields. Many interesting features learned from peptide self-organisation and hierarchical templating will serve as useful guidance for functional materials design and nanobiotechnology (123 references).

1. Introduction

Molecular self-assembly describes the spontaneous organisation of molecules into bigger and structured arrangements. In the bio-world, molecular self-assembly is ubiquitous and the assembled entities have their unique biological functions. Studying molecular self-assembly is critical to the current endeavour of nanotechnology because this process provides guidance on designing the molecular building blocks that can trigger spontaneous and stepwise interactions and assemblies. Nature started the evolution of biomolecules from the primitive ones through countless iterations of self-assembly and disassembly and ultimately produced an enormous amount of complex but intriguing biomolecular systems. What is hence inspiring to us is the design of chemically complementary and structurally compatible constituents for biomolecular self-assembly through natural selection and evolution.

A few decades ago, the constituents of biological origins such as amino acids and nucleotides were not generally considered to be useful building blocks for materials engineering. This concept has since changed rapidly with the recent development of biotechnology, genetic engineering, synthetic and materials chemistry. Tremendous advances have been made over the past 15 years in the use of peptides, phospholipids and DNA as building blocks, and molecular self-assembly is now widely regarded as an important route to produce novel materials to cover a wide and unique range of applications. Biomimetic and bioinspired biomaterial research is now emerging as an important and fast developing field.

Designing and synthesizing molecules that self-assemble into well ordered nanostructures is an attractive “bottom-up” approach for developing new functional nanobiomaterials for nanoscience, nanotechnology and nanomedicine.^{1,2} Molecular evolution over billions of years has produced elegant biomolecular self-assembly systems such as lipid bilayers and vesicles as barriers or containers for sub-cellular organelles, highly ordered polymeric nucleic acids as genetic information carriers, 3D polypeptides and proteins as ion pumps and action executors.³ To design, fabricate and construct better and functional materials beyond Nature, we need not only inspirations from Nature but also the knowledge learned from simple and exquisite molecular structures. Extensive research activities over the past decade have been devoted to the design and fabrication of novel biomimetic nanobiomaterials through peptide self-assembly.⁴ Many synthetic peptides have recently been explored as useful nanobiomaterials in applications ranging from drug release,⁵ gene delivery,⁶ membrane protein stabilisation⁷ to 3D cell culture and tissue engineering^{8–18} due

^a Biological Physics Laboratory, School of Physics and Astronomy, University of Manchester, Schuster Building, Oxford Road, Manchester, UK M13 9PL. E-mail: J.Lu@manchester.ac.uk; Tel: +44 161-306-3926

^b National Key Lab for Heavy Oil Processing and Center for Bioengineering and Biotechnology, China University of Petroleum, Qingdao, Shandong 266555, China. E-mail: xuh@upc.edu.cn; Tel: +86 532-86981318

^c Institute of Bioengineering and Nanotechnology, A*STAR, 31 Biopolis Way, The NANOS, 138669 Singapore. E-mail: chauser@ibn.a-star.edu.sg; Tel: +65 6824-7108

^d Center for Biomedical Engineering NE47-379, Center for Bits & Atoms, Massachusetts Institute of Technology, 77 Massachusetts Avenue, Cambridge, MA 02139, USA. E-mail: Shuguang@mit.edu; Fax: +1 617-258-5239; Tel: +1 617-258-7514

† Part of the peptide- and protein-based materials themed issue.

to their excellent functions and biocompatibility. In addition to being benign to mammalian cells, some of these short peptides have been investigated as antimicrobial agents due to their excellent selectivity against different membrane structure and composition.^{19,20} The time for building and utilising functional nanobiomaterials from a bottom-up approach is now truly coming.²¹

Peptides that have been reported so far vary enormously in molecular size and structure. They can be biomimetic or *de novo* designed. This review aims to outline recent advances in the design and application of short peptide amphiphiles and lipopeptides, focusing on the nanostructures formed by them and the factors affecting their nanostructure formation. Representative peptides to be covered in this review are listed



Top (left to right): Xiubo Zhao, Fang Pan, Hai Xu and Mohammed Yaseen. Bottom (left to right): Honghong Shan, Charlotte A. E. Hauser, Shuguang Zhang and Jian R. Lu

Xiubo Zhao received his BEng degree (2003) in biochemical engineering from China and his PhD degree (2006) in biological physics from the University of Manchester. He is currently an EPSRC funded research associate in the Biological Physics Group at the University of Manchester. His research interests include peptide self-assembly; non-viral gene delivery; interfacial adsorption of biomolecules; biomarker immobilization and detection for bio-sensing; antimicrobial and anti-wrinkle peptides; biomaterials, biocompatible surfaces and antifouling.

Fang Pan received her B.M. degree From YangZhou University in 2004 and her PhD degree in biological physics from the University of Manchester in 2009. She is currently a research associate in the Biological Physics Group at the University of Manchester. Her research interests include peptide self-assembly; non-viral gene delivery; antimicrobial and anti-wrinkle peptides; biomaterials, biocompatible and thermoresponsive polymers for tissue engineering.

Hai Xu, born in Shandong, China, in 1971, received his PhD in chemical engineering from China University of Petroleum (UPC) in 2002. He then spent three years working as a research associate in the Biological Physics Group led by Prof. Jian R. Lu, at the University of Manchester. He is currently a professor in the Centre for Bioengineering and Biotechnology, UPC. His research interests include the design and synthesis of novel molecules with cellular origin, their self-assembly and nanostructuring in aqueous solution and at interfaces, and their application in biomimetic synthesis of functional materials and nanomedicine.

Mohammed Yaseen obtained his first degree in Chemistry from Edinburgh University (UK). In 2003 he obtained his PhD in Biological Physics from the University of Manchester Institute of Science and Technology. He is presently a research associate at the University of Manchester. His scientific interests include biomaterials, surface modification and interactions by nanoparticles, polypeptides, proteins and cells. Further interests include biosurfactant synthesis, neutron reflectivity and more recently the development of carbon nanotubes and magnetic nanoparticles for biomedical applications.

Honghong Shan, born in Henan, China, in 1959, obtained her PhD in chemical engineering from China University of Petroleum (UPC). She is currently a Professor in the College of Chemistry and Chemical Engineering, UPC and leads an interdisciplinary group to develop chemical conversion technologies of oil and renewable resources. Her research also focuses on the design, synthesis, and industrial applications of novel catalysts and nanomaterials, and chemical reaction engineering.

Charlotte Hauser is a Team Leader and Principal Research Scientist at the Institute of Bioengineering and Nanotechnology (IBN) in Singapore. She did her PhD studies at the Massachusetts Institute of Technology (MIT), Cambridge, USA. She was a Research Fellow at the Institute National de la Santé et de la Recherche Médicale (INSERM) in Paris, France, and led a research group at the Max-Planck-Institute (MPI) of Psychiatry in Munich, Germany. She founded life science company Octagene, Martinsried, Germany, now with Octapharma AG, and was managing director and share holder (1997–2006). She holds numerous scientific articles, patents and awards.

Shuguang Zhang earned his PhD in Biochemistry & Molecular Biology from University of California at Santa Barbara. He has published > 140 papers in protein science and nanobiotechnology from designer self-assembling peptides and studies into membrane proteins for emerging biosolar energy. He was an American Cancer Society Postdoctoral Fellow and a Whitaker Foundation Investigator at MIT. He is a distinguished Chang Jiang scholar in China and a 2003 Fellow of Japan Society for Promotion of Science. His work on designer peptide scaffolds won 2004 R&D100 award. He was a 2006 John Simon Guggenheim Fellow and a winner of 2006 Wilhelm Exner Medal of Austria.

Jian Ren Lu is a Professor and Head of Biological Physics, School of Physics and Astronomy at the University of Manchester. He obtained his PhD in surface chemistry at the University of Hull in 1991 and then undertook a five year post-doctoral research post in Physical and Theoretical Chemistry at the University of Oxford to develop neutron and X-ray reflection for studying wet interfaces. His research focuses on self-assembly of lipids, small peptides, surfactants, proteins, polymers and their mixtures at interface and in solution and has published extensively on mechanistic processes of self-assembly and molecular implications of surface biocompatibility.

Table 1 Summary of peptide amphiphiles incorporated in this review

Primary peptide sequences	Assembled nanostructures	Applications	Reference numbers
Ac-A _m K-NH ₂	Nanorods, nanotubes, bilayers	Antimicrobial agents and stabilisation of membrane proteins	7, 20, 30–37
Ac-V _m K _n -NH ₂	Bilayers, nanotubes, nanovesicles	DNA immobilisation and stabilisation of membrane proteins	34, 35, 38
Ac-G _m D _n -OH	Nanotubes, nanovesicles		39
Ac-A ₆ D-OH	Nanoropes, nanotubes, nanovesicles	Nanofabrication	7, 33, 34, 36, 37, 40, 41
Ac-V ₆ D-OH	Nanotubes, nanovesicles	Stabilisation of membrane proteins	7, 31, 32, 40, 41
Ac-KA ₆ -OH	Nanotubes, nanovesicles	Stabilisation of membrane proteins	34, 37
Ac-GAVILRR-NH ₂	Nanodoughnuts, spherical micelles	Nanofabrication	42
Ac-I ₃ K-NH ₂	Nanotubes	Templates for silicification	43
Ac-L ₃ K-NH ₂	Nanovesicles		43
K _m L _n	Nanofibrils and gels	Foods, cosmetics and drug delivery	44–46
NH ₂ -X ₅ -H ₄ R ₈ -CONH ₂ (X = I, W, F)	Nanoparticles	Gene delivery	47
Chol-H _{50or10} R ₁₀	Core-shell nanomicelles	Gene delivery	48
Ac-(AF) ₆ -H ₃ K ₁₅ -NH ₂	Core-shell nanomicelles	Gene and drug delivery	49
A ₁₂ H ₅ K _{10or15}	Core-shell nanoparticles	Gene delivery	50
Ac-A ₂ V ₂ L ₃ WE _{2or7} -COOH	Spherical nanovesicles	Potential drug delivery vehicles	51
C ₁₂ H ₂₃ -EVHHQKL	Nanofibrils	Potential use in bio-fabrication	52
C ₁₆ H ₃₁ -C ₄ G ₃ S ^(PO₄) RGD	Nanofibers	Mineralisation	53, 54
C ₁₀ H ₁₉ -A ₄ G ₃ S ^(PO₄) RGD	Nanofibers	pH responsive scaffolds	53
C ₁₆ H ₃₁ -A ₄ G ₃ EIKVAV-OH	Nanofibers	Nanofabrication	55
C ₁₆ H ₃₁ -A ₄ K ₄	Nanofibers	Templates for silicification	56
C ₁₀ H ₁₉ -C ₄ G ₃ S ^(PO₄) RGD	Nanofibers	pH responsive scaffolds	53
C ₁₆ H ₃₁ -W(A ₄ K) ₃ A	Spherical, worm-like micelles, nanofibers	Scaffolds	57
C ₁₆ H ₃₁ -O-VEVE	Nanobelts, nanoribbons	pH responsive materials	58
C ₁₆ H ₃₁ -V ₃ A ₃ E ₃	Nanofibrillar gels	Cell culture scaffolds	59, 60
C ₁₆ H ₃₁ -V ₃ A ₃ K ₃ RGDS	Nanofibrillar gels	Cell culture scaffolds	60, 61
Fmoc-RGD	Hydrogels	Cell culture scaffolds	11
C ₁₆ H ₃₁ -KXX (X = A, G, L, K)	Nanofibrils and nanomicelles	Antimicrobial agents	62
C ₁₆ H ₃₁ -LSQETFSDLWKLLPEN	Rod-like micelles	Inhibit p53-MDM2 protein interaction	63
C ₁₆ H ₃₁ -GTAGLIGQERGD	Long nanofibers	Cell adhesion, migration and drug delivery	64, 65
Chol-G ₃ R ₆ YGRKKRRQRRR	Nanoparticles	Antimicrobial agent	66
RGDSKLLA(K)-C ₈ H ₁₆ -diacetylene-	Nanofibers	Nano patterning, Cell culture scaffold	67
C ₁₂ H ₂₅			
C ₁₆ H ₃₁ -KTTKS		Anti-wrinkle	68
C ₁₆ H ₃₁ -GQPR		Anti-wrinkle	69
C ₁₆ H ₃₁ -GHK		Anti-wrinkle	69
Ac-AO(C ₁₄ H ₂₇)AEEAAEKAAY-		Stabilise membrane proteins	70
AEEAAEKAAKAO(C ₁₄ H ₂₇)A-NH ₂			

in Table 1. Where relevant, we also highlight the technological applications of these novel peptide molecules. We note that a number of other reviews have already introduced other types of peptides, peptide-polymer conjugates or general biomimetic materials.^{1–3,22–29}

2. Design of peptide amphiphiles

2.1 Amino acids as building blocks

Nature provides some 20 amino acids as building blocks for constructing peptides and proteins. All of them are chiral molecules (except glycine) with similar structures but bearing different side groups (R). It is the difference within the R groups that enables the molecules to bear different properties and biological functions. Accordingly, amino acids can be divided into different categories such as polar, non-polar, aliphatic, positively or negatively charged, aromatic, *etc.*^{3,71,72} This range of variations makes it possible to produce an enormous number of peptides and proteins with different biological functions through the combination of different amino acid sequences and lengths.

Structural complementarity and local interactions readily drive the formation of secondary structures such as α -helix and β -sheet conformations. Although hydrogen bonding is ubiquitous in peptides and proteins,^{73–77} hydrophobic affinity^{33,35,36,39,42,78} (aliphatic residues) and π - π stacking^{3,79–82} (aromatic residues) between residues are instrumental in both peptide self-assembly and stabilisation of the secondary structures and the subsequent tertiary structures for the proteins. In a globular protein structure, charged residues are normally exposed to the outer surface offering favourable interactions with water. Whilst the presence of charged groups provides selective responses to other charged molecules or surfaces, these responses can be tuned by solution pH as well as ionic strength. Thus, hydrogen bonding, electrostatic and hydrophobic interactions together need to be taken into account when studying peptide self-assembly.^{24,73,83} However, these interactions are mostly weak. Many of the self-assembled materials show sensitive responses to environmental conditions such as pH, temperature, ionic strength, different ions, light.⁶⁴ Certain residues have unique functions in the assembly/folding systems. Proline (P), for example, has

conformational rigidity compared to other amino acids. It is commonly found in turns such as hairpins or at the beginning of an α -helix and also in the edge strands of a β -sheet. This advantage has been utilised for intramolecular folding in peptide self-assembly.^{24,84} A large body of work using proline to make hairpin peptides (such as $(VK)_4V^D$ PPT- $(KV)_4$ -NH₂) has been carried out by Schneider *et al.*^{85–92} These self-assembling peptide hydrogels have been used for drug release and cell culture.^{87,90–93} Some of them also have antibacterial activity.^{85,94} In another example, cysteine (C) provides a reactive thiol side chain for disulfide cross-linking and chemical modification.⁵⁴ It also participates in enzymatic reactions and binding on gold surfaces.³ Tyrosine (Y), serine (S) and threonine (T) can also be utilised for chemical modification.³ These hydroxyl group-containing amino acids play important roles in moisture keeping for cosmetic applications.

2.2 Designing strategies

Self-assembling peptides have been designed to form different structured aggregates such as nanofibers, nanovesicles, nanobelts, and nanotubes.⁹⁵ Peptide amphiphiles represent a simple category of the designed self-assembling peptides. Both the structure and the chemical properties of these peptides bear the lipid or surfactant characteristics. They possess a hydrophobic tail and a hydrophilic head (Fig. 1). They mostly have well defined critical aggregation concentrations (CAC),^{33,36,41,42} and can self-assemble in aqueous solution and at interfaces to form well-ordered nanostructures including peptide bilayers, nanotubes, nanorods, nanovesicles and micelles.^{30,35,36,39–41,96}

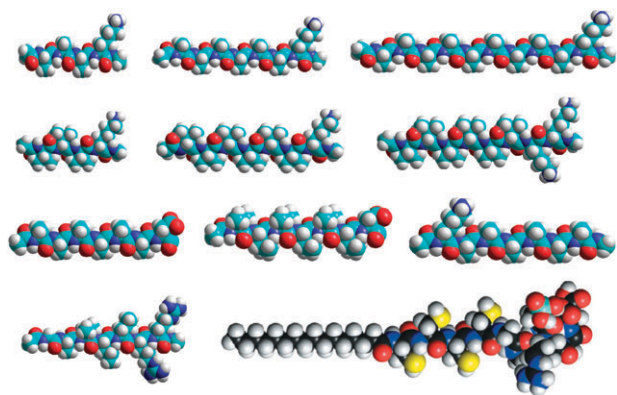


Fig. 1 Examples of designer peptide amphiphiles. They are (from left to right and top to bottom): Ac-A₃K-NH₂, Ac-A₆K-NH₂, Ac-A₉K-NH₂, Ac-V₃K-NH₂, Ac-V₆K-NH₂, Ac-V₆K₂-NH₂, Ac-A₆D-OH, Ac-V₆D-OH, Ac-KA₆-OH, Ac-GAVILRR-NH₂, C₁₆H₃₁-C₄G₃S^(PO₄)RGD. Each one has different CAC and self-assembles differently in water. The dislike of the hydrophobic peptide tails to water drives aggregation to form nanovesicles, nanotubes, nanofibrillar networks, or membrane sheets with their tails buried inside the core and their hydrophilic heads exposed to water. The hydrophobic tails can be made from non-polar amino acid residues (e.g. G, A, V, F, P, I, L) or acyl chains. The hydrophilic heads can be made from charged amino acid residues such as net negative (D, E), net positive (H, K, R), or a mixture of positive and negative residues. (The last molecule was adapted from *Science*, 2001, **294**, 1684. Copyright © 2001 American Association for the Advancement of Science.)

The tails of peptide amphiphiles are normally composed of non-polar amino acid residues (G, A, V, I, L, P and F). These amino acids have different size, shape and hydrophobicity. Meanwhile, the tails can also be made of hydrocarbon chains or even a mixture of hydrocarbon chain and non-polar amino acids. One hydrocarbon chain (or more) is connected to a hydrophilic peptide sequence to form a category of molecules called lipopeptides. The hydrophilic heads of these molecules can also be positively charged (H, K and R), negatively charged (D and E) or contain a combination of both of them.

In a peptide amphiphile, the hydrophobic tail normally contains 3–9 hydrophobic amino acids or 12–16 carbons in an acyl chain. The longer the tail the poorer the solubility it has. On the other hand, with decreasing tail length, the solubility increases and the tendency for aggregation decreases. Decrease in tail length can however be balanced by increase in the size of hydrophobic amino acids or branching in the acyl chain. Examples of different peptides are given in Fig. 1. For these peptide amphiphiles, both peptide tail length and cross-sectional diameter affect their hydrophobicity. The head often bears one or more charges and can be either positive or negative.^{39,40} Note that for the normal N–C type of sequences, most designed peptides have their hydrophobic moiety on the N end and hydrophilic moiety on the C end. The terminal charge on the N end is usually blocked by an acetyl group whilst the carboxylic group on the C terminal is either blocked by an amine group, or left open. However, the two amphiphilic moieties can be swapped around, with the hydrophilic head located at the N end and the hydrophobic tail at the C end (e.g. KA₆(KAAAAA-NH₂)).³⁵ The implication of this type of rearrangement of the amphiphilic moieties to nanostructure seems not great. But because of the location of the charged groups, charge associated function can be very different. The total lengths of these peptides are normally around 3 nm, similar to the lengths of phosphatidylcholine lipid molecules. Lipopeptides may have longer lengths, depending on the peptide sequences and the tails chosen. Well-ordered nanostructures can be formed through self-assembly when the concentrations are above their CAC, below which no defined nanostructures can be observed.^{33,36,41} These characteristics are broadly similar to conventional lipids and surfactants. However, the structural differences between peptide sequence and acyl chain may cause different interactions and structural consequences. Furthermore, many bio-functional groups such as biotin and cell adhesion epitopes such as RGDS have been incorporated into the peptide amphiphiles for biological applications.^{61,97,98} Whilst these bioactive groups bring in new functions, they must also have direct implications to nanostructural formation.

3. Self-assembly of peptide amphiphiles

3.1 Synthetic peptide amphiphiles

Nanostructures formed by self-assembling peptide amphiphiles. Self-assembled nanotubes, nanofibers and nanovesicles have been reported using both cationic and anionic peptides.^{35,39–41,99} Peptides such as G_nD₂, A₆D, V₆D and

V_6D_2 have two or three negative charges at the C termini (with the terminal carboxylic acid group unblocked) with glycine (G), alanine (A) or valine (V) as tails. Two size distributions of the nanotubular structure were formed from the self-assembly of G_nD_2-OH peptide. The dimensions of the small structure are 40–80 nm while the sizes of the big structure are in the order of 100–200 nm. Peptides with alanine and valine tails form more homogeneous and stable nanostructures than those of glycine, isoleucine and leucine.²² A typical example of the nanotubes formed by the $Ac-V_6D-OH$ peptide is shown in Fig. 2A. The clear contrast at the end confirms the tubular structure. The V tails are thought to pack back to back to form a bilayer as the wall of the nanotube through hydrophobic interaction with the charged groups outside facing the water phase. Nanovesicles also form in

the system. Similar structures have been reported from other peptide amphiphiles such as the trifluoroacetate salt of A_6K^{100} and I_3K ($Ac-I_3K-NH_2$). Results from cryo-transmission electron microscopy (cryo-TEM) and small-angle X-ray scattering (SAXS) demonstrated that A_6K peptide formed hollow tube structure with diameters of 25–30 nm. In a different study of A_6K with small Cl^- counterions, the diameters of A_6K nanotubes were found to be about 7–8 nm.¹⁰⁰ The difference could be attributed to the different extent of affinity and charge interaction arising from the two counterions. Shorter peptide I_3K formed nanotubes with diameters about 10 nm and lengths over 5 μm . The nanostructure from this ultra-short peptide clearly indicates that the amphiphilicity of a peptide amphiphile can be balanced between the length of a peptide sequence and the size of hydrophobic

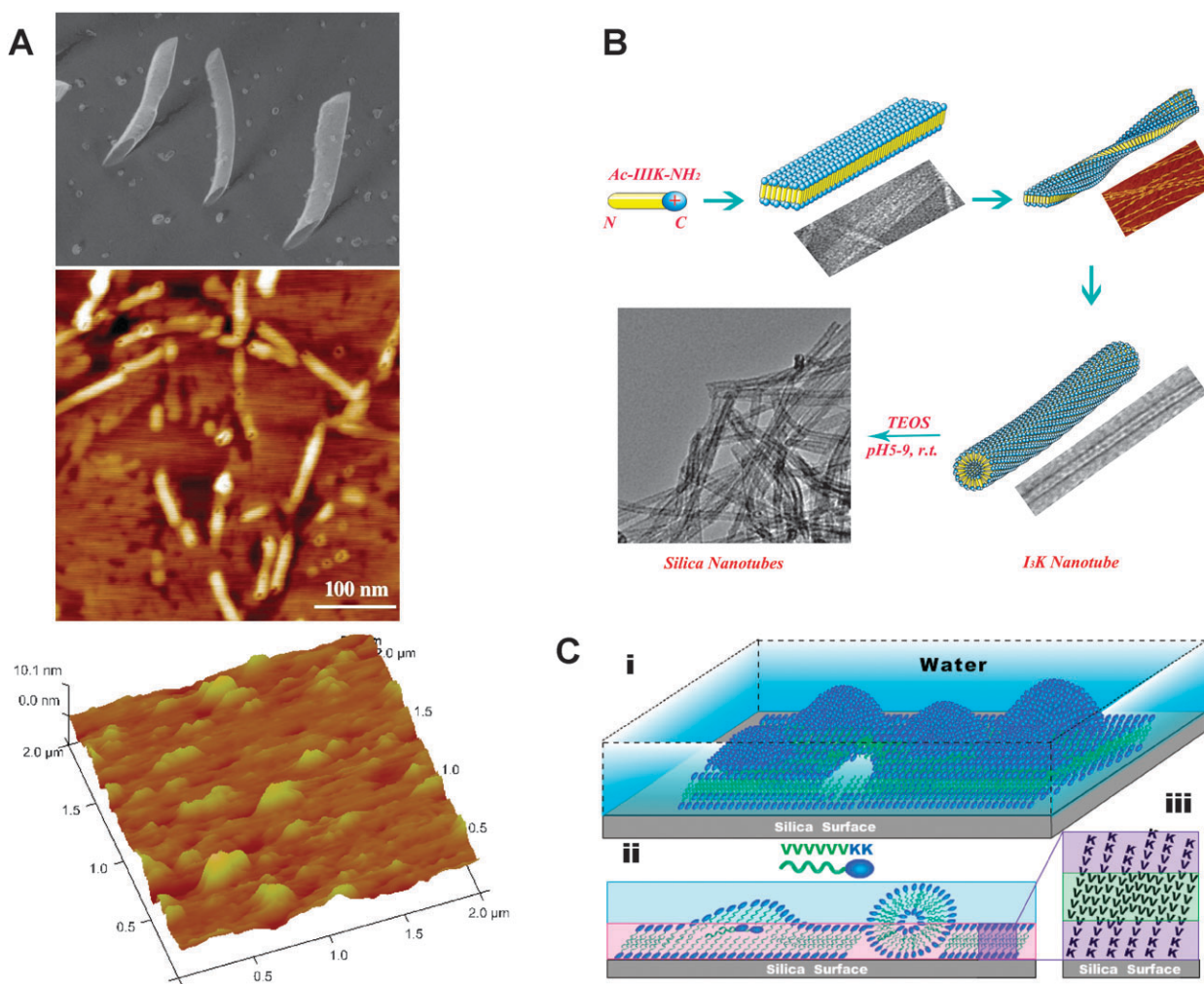


Fig. 2 TEM and AFM images of self-assembled nanostructures formed from designer peptides. (A) Top, a Quick-freeze/deep-etch TEM image of $Ac-V_6D-OH$ dissolved in water (4.3 mM at pH 7), shows the diameters of 30–50 nm with clear openings on nanotube ends. Bottom, an AFM image of nanotubes formed from peptide $Ac-A_6K-NH_2$, also with openings at the ends of the nanotubes. B, A schematic representation of I_3K self-assembly process leading to the formation of peptide nanotubes which can then serve as templates for silicification. C, Left, AFM image of a membrane bilayer formed by peptide $Ac-V_6K_2-NH_2$ at the silica/water interface. Vertical section analysis indicates that the thickness of the peptide bilayer is about 4 nm, incorporated with small vesicular blobs with thickness around 8 nm. Right, schematic cartoon models to indicate the structure of the peptide interface at the silica/water interface: (i) An overall in-plane morphology of the adsorbed peptide structure showing a predominant peptide bilayer incorporating a few vesicles and defects, (ii) Typical vertical sectioning of the peptide layer, (iii) The detailed molecular packing structure in the dense bilayer region. (A was adapted from *Nano Today* 2009, 4, 193. Copyright © 2009 Elsevier Ltd. C was adapted from *Soft Matter* 2009, 5, 1630. Copyright © 2009 The Royal Society of Chemistry.)

amino acids.⁴³ Again, I₃K molecules are thought to initially interdigitate with each other through the hydrophobic interaction between the I₃ tails to form bilayer fragments. The self-assembly is driven by the hydrophobic affinity between isoleucine residues with the I₃ tails packed in the middle and the K residues projected at the outside facing water. The peptide bilayer fragments then further assemble into twisted ribbons. The fusion of the helical ribbons results in the formation of stable nanotubes, indicating the strong driving force along the main axial direction of the nanotubular structure (Fig. 2B). The enormously long nanostructures also demonstrated high stability against heating and exposure to organic solvents such as ethanol. The stable I₃K nanotubes were also successfully used as templates for silicification to form silica nanotubes.

While the peptide molecules form well-ordered nanostructures in bulk solution, it is also useful to characterise their interfacial structures and mechanistic processes of interfacial structuring due to the direct relevance to practical applications. Atomic force microscopy (AFM) and neutron reflection (NR) have been used to unravel the interfacial structure formed from adsorption of V₆K₂ (Ac–V₆K₂–NH₂) at the SiO₂/water interface.⁹⁶ As depicted in Fig. 2C, interfacial adsorption led to the formation of a predominant peptide bilayer that broadly resembles a lipid membrane bilayer. In addition, some large vesicular blobs and structural defects are also incorporated into the bilayer structure. Similar membrane bilayer structures were also observed from the self-assembly of A₆K (Ac–A₆K–NH₂). The bilayer formation was also confirmed on freshly cleaved mica surfaces (Fig. 2A).

In an effort to obtain detailed structural information about the V₆K₂ adsorbed interface, NR was used to determine the V₆K₂ peptide adsorption under solution conditions similar to those used in AFM measurements. To improve interfacial structural resolution, both fully hydrogenated sample hV₆hK₂ and partial deuterium labelled dV₆hK₂ (tail deuterated sample) were used.^{96,101} The different labelling thereby provided a sharp isotopic contrast for highlighting the hydrophobic tail region. It was found that the peptides formed a dense layer with a thickness around 4 nm containing about 50% peptide. However, this dense layer region also contained defects, as evident from AFM imaging. A further 4 nm was required to account for the loose outer layer containing some 8% peptide on the solution side. Further NR measurements under different isotopic contrasts (*e.g.* under D₂O) were also undertaken to highlight the interfacial structure differently. The combined NR profiles led to a detailed structure of the membrane-like bilayer as revealed in Fig. 2C.⁹⁶ The basic bilayer feature for the dense packed peptide inner region was demonstrated by the need of the sandwiched molecular packing at the interface to fit all the reflectivity profiles. The actual bilayer was comprised of a sandwiched hydrophobic tail region (V₆) interdigitated to each other and the two almost symmetrical cationic head group regions (K₂) projected towards the oxide surface and the bulk water. The middle hydrophobic V tail region had a thickness of 1.4–1.6 nm containing more than 50% peptide. Each of the two outer head regions had the thickness around 1.1–1.3 nm and contained less peptide. The formation of the peptide bilayer

structure was clearly due to the strong amphiphilic nature of the peptide molecules. Similar symmetrical bilayer structure has also been observed by the interfacial assembly of V₆K peptide.³⁸ The AFM and NR measurements demonstrated that the membrane-like bilayer formed by V₆K was smoother, without any large vesicular blobs being incorporated. The adsorption of this interfacial bilayer also displayed a distinct trend of salt effect. The addition of NaCl not only reduced the surface adsorbed amount of V₆K but also slowed down adsorption dynamics. Furthermore, the membrane-like bilayers formed by both V₆K₂ and V₆K showed interesting ability for DNA immobilization. DNA molecules only became bound or associated with the outer leaf of the membrane-like surface. Thus the charge interaction between the outer bilayer surface and DNA must be responsible for driving the binding interfacial event.³⁸

Structure effect. Many intriguing nanostructures have been reported from self-assembly of different peptides. However, it is still not well understood why and how these structurally different peptides form so many differently shaped nano-assemblies. What are the key factors that affect the nanostructure formation in terms of size, shape and stability? How can we control these nanofabrication processes? Clearly, peptide sequence and length are critically important. Further studies are needed before we can answer these basic questions. For peptide amphiphiles, however, some very interesting observations have already been made, showing how the balance of hydrophilicity and hydrophobicity, the lengths of the tail and head and the geometrical constraints of the peptide molecules can affect nanostructures.^{42,45}

An interesting example of the effect of the molecular geometry on nanostructure formation can be seen from the doughnut-shaped nanostructure as shown in Fig. 3A, where the design of a cone-shaped peptide amphiphile led to the formation of the coexistent shapes of nano-sphere and nano-doughnut.⁴² The molecule Ac–GAVILRR–NH₂ was designed to have a hydrophobic tail with increasing hydrophobicity with side-chain size (GAVIL) and a large cationic head group composed of two arginine amino acids (R), thereby a cone-shaped molecular structure. Its CAC was 0.82 mM in water and 0.45 mM in phosphate buffered saline (PBS). Formation of both vesicular and doughnut-shaped nanostructures was observed at concentrations above CAC. From structural analysis and model fitting, the outer and inner diameters of the doughnut-shaped nanostructures estimated to be around 110 nm and 25 nm, respectively. The average thickness of the doughnut-shaped structures is around 41.5 nm, similar to the diameter of the spherical nano-vesicles. It was proposed that a plausible self-assembling pathway leading to the formation of the nano-doughnut structure was the self-assembly through fusion or elongation of short spherical micelles that merge together side by side, and that then bend and fuse to form the nano-doughnut structure. The bending arises from the tension inherent of the packing and interaction of the cone-shaped peptide side-chains.² These observations are not only useful for further molecular design but also important to the understanding of peptide self-assembling mechanisms. Similar cone-shaped peptide amphiphiles have also been designed and

reported by van Hell *et al.*⁵¹ Instead of the solid-phase synthesis, the DNA sequence was designed and transformed into an *E. coli* strain. Peptide amphiphiles Ac-A₂V₂L₃WE_{2or7}-COOH was recombinantly produced from the bacterial culture. The CAC values were found to be 4.9×10^{-4} mM for Ac-A₂V₂L₃WE₂-COOH and 1.6×10^{-2} mM for Ac-A₂V₂L₃WE₇-COOH, respectively. Spherical nano-vesicles with radii ~ 60 nm were found by the self-assembly of the two peptide amphiphiles above their CACs. The nano-assemblies started to form around pH 5. The pH dependent assembling process was found to be fully reversible. Efficient encapsulation of calcein molecules into the nano-vesicles suggested that

the self-assembling systems could be used as pH-dependent drug delivery vehicles.

Another example of the effect of molecular structure on nanostructure formation is the A_mK peptide series. Peptides Ac-A_mK-NH₂ ($m = 3, 6$ and 9) showed a steady transition of size and shape of nanostructures with increasing hydrophobic tail length m .^{30,102} The CACs of these peptide amphiphiles decreased with increasing hydrophobic tail length. Up to the peptide concentration of 4 mM, the highest concentration studied, no distinct CAC was found for A₃K, possibly due to its weak hydrophobicity. The CACs for A₆K and A₉K in water were 0.2 mM and 0.015 mM, respectively. It was

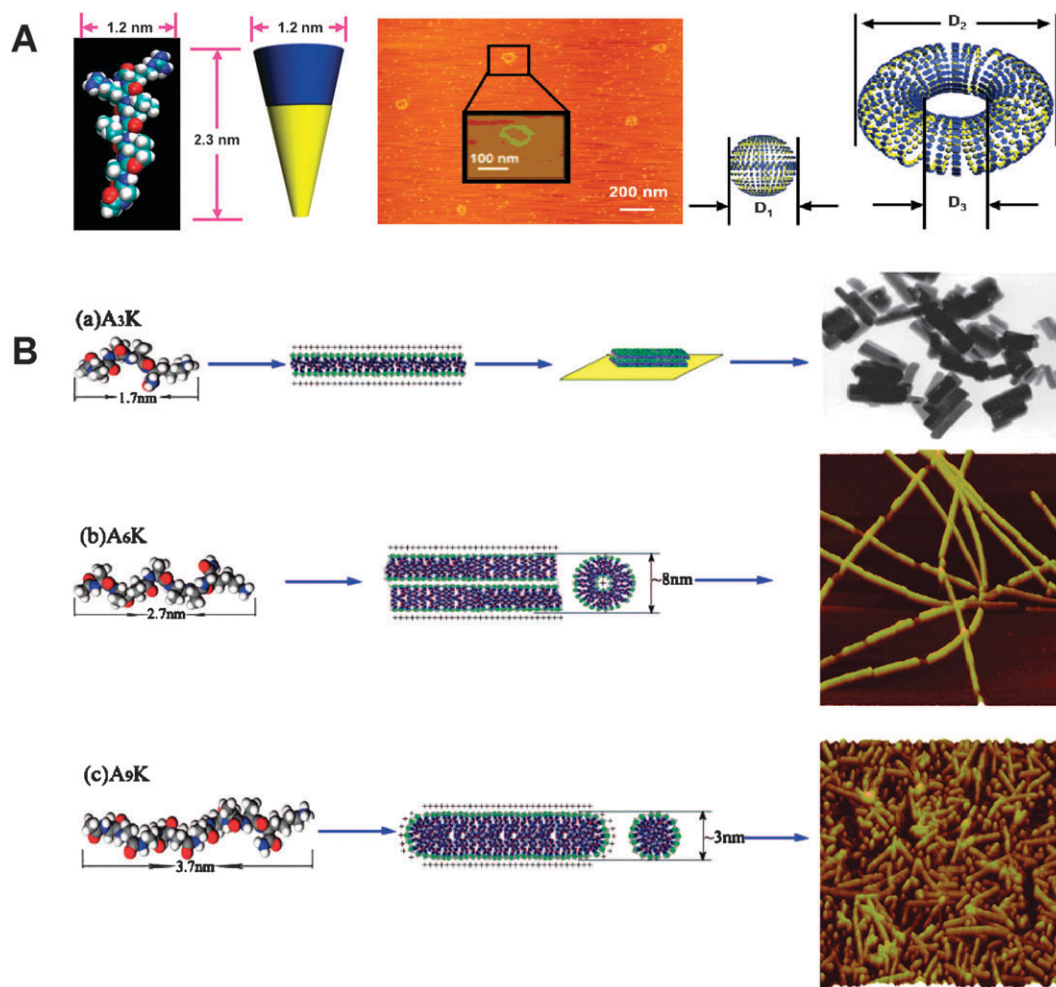


Fig. 3 A, molecular model of Ac-GAVILRR-NH₂ (left). The peptide is approximately 2.3 nm long and 1.2 nm wide (colour code: hydrogen = white, carbon = cyan, oxygen = red and nitrogen = blue). The cone-shaped model is simplified for the shape of Ac-GAVILRR-NH₂. The blue part indicates the positively charged hydrophilic region and the yellow part indicates the hydrophobic region. AFM image for the aggregate structures of Ac-GAVILRR-NH₂ in water at the concentration of 1 mM (middle) indicates the coexistence of nano-doughnut structures and the spherical micelles. The inset shows a zoomed image of the doughnut-shape structure. Schematic illustrations of the structures of the spherical micelle and the nano-doughnut are displayed on the right. The average diameter of the micelles ($D_1 = \sim 40$ nm) and the outer and inner diameters of the nano-doughnut structure ($D_2 = \sim 110$ nm; $D_3 = \sim 27$ nm) are obtained from section analysis of tens of nano-doughnuts in different AFM images. B, Schematic illustrations of Ac-A_mK-NH₂ peptide self-assembly. (a) A₃K has the shortest chain and has no apparent CAC detected, giving rise to the lowest effective a_e and the highest packing parameter; consequently, stacked A₃K bilayers are formed. (b) With increasing hydrophobic tail length and decreasing CAC of A₆K, the electrostatic repulsion between the head groups increases. This, together with the packing and entropic effect, leads to the lowering of the packing parameter and the formation of nanofibers. (c) A₉K has the lowest CAC, the highest electrostatic repulsion between head groups, and the largest entropic effect arising from the longest tail, resulting in the formation of nanorods. In each case, lysine (K) groups remain at the outer surface of the nanostructures formed. (Reproduced from *Langmuir* 2009, **25**, 4111 and 4115. Copyright © 2009 American Chemical Society.)

subsequently found that A₃K formed unstable peptide sheet stacks. A₆K formed long nanotubes or nanofibrils while A₉K self-assembled into short nanorods (Fig. 3B). The fibers formed by A₆K had uniform diameters (6–8 nm) with long and flexible lengths over 1 μm. These long nanofibers could become weakly interweaved. In comparison, the nanorods formed by A₉K had smaller diameters around 3 ± 1 nm and were much shorter, with lengths typically less than 100 nm. The trend in the variation of the size and shape of the peptide aggregates can be accounted for using the packing parameter concept for common surfactants. Increase in the length of the tail results in the changes of packing style within peptide nanostructure and the decrease in CAC. The transition from sheet stacks to nanofibrils or nanotubes and finally to short nanorods results from the gradual increase in spontaneous curvature relating to the entropic effect inherent of chain packing and the increased electrostatic repulsion.

Work by Deming *et al.* has also demonstrated that the length of the hydrophobic tail affects the formation of nanofibrillar structures and the subsequent gel formation.^{44,45,103} In their studies, they used diblock and triblock peptide copolymers instead of small peptide amphiphiles like A_mK series studied by us. Peptides with short tails (such as K₁₉₀L₁₀) did not form gels even at high concentrations, while increase in the tail length and decrease in the head length resulted in the reduction of gelation concentration, showing a clear and consistent need for amphiphilic balance in these macromolecules.

These examples, though limited, are sufficient to illustrate a clear relationship between molecular geometry and the size and shape of the nano-objects formed. As in the case of surfactants, however, the precise nanostructure of a peptide amphiphile and its structural transition will respond sensitively to other factors such as electrostatic interactions relating to solution pH and ionic strength.

Dynamic process. Further experiments demonstrated that the molecular self-assembly of A₆K peptide is a dynamic process (Fig. 4). Aggregated peptide stacks were formed during the first hour of solution preparation, followed by their assembly into short nanofibrillar segments from the subsequent few hours to the 24-hour period. An interesting observation of alignment of short nanofibers into mature long ones then occurred, with final lengths extended to several microns but with diameters remaining fixed at 6–8 nm. Even after a week, gaps or joints still remained in the mature nanofibers, reminiscent of an imperfect self-healing process under the experimental conditions. The final A₆K nanofibers looked like strings of sausage rolls. The formation of A₆K nanofibers was confirmed by parallel small angle neutron scattering (SANS) with comparable diameters obtained. SANS measurements showed a high sensitivity to the slight change in diameter. It was however less sensitive to the length of the nanofibers. This meant that when SANS was used to follow the dynamic growth of A₆K nanofibers, its scattering intensity profiles changed little with time, which was exactly what was observed. In contrast, A₉K self-assembled into smaller nanorods quickly. The entire self-assembling process

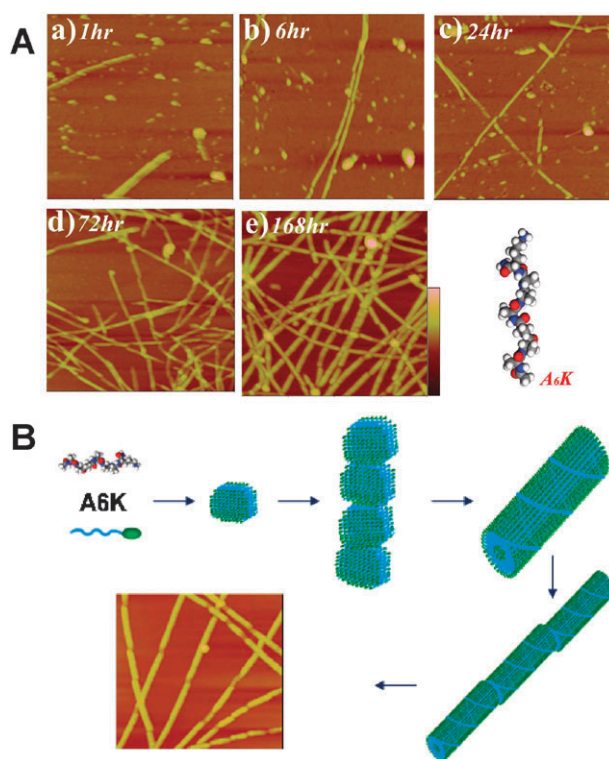


Fig. 4 A, 1 μm × 1 μm AFM topographical images of A₆K assemblies (2 mM at pH 6.0) at different time points: (a), 1 h; (b), 6 h; (c), 24 h; (d), 72 h; and (e), 168 h. The Z scale for all images is 15 nm as indicated. B, schematic illustrations of the dynamic self-assembly process and nanostructures formed for A₆K in aqueous buffer. (Adapted from *Soft Matter* 2009, 5, 3870. Copyright © 2009 The Royal Society of Chemistry.)

completed within the first hour and there were little further morphological variations afterwards.¹⁰²

Synergistic effect. Synergistic effects in the context of this review refer to the changes in the solution aggregation and interfacial behaviour that are beyond what are expected from the usual variations of molecular structure or solution conditions. As shown in Fig. 5,³³ the mixing of Ac–A₆D–OH and Ac–A₆K–NH₂ led to the occurrence of the unusually low CACs and the formation of the various assembled nanostructures. The two peptides had their CACs at 0.46 mM and 0.93 mM in water, respectively.³³ The CAC varied with the ratios of the two peptides, with the lowest CAC values being obtained for Ac–A₆D–OH/Ac–A₆K–NH₂ = 1:2 in both water and PBS solutions. The neutralisation of the oppositely charges between the two peptides was clearly responsible for substantially reduced CACs.³³ Various nanoropes and nanorods were observed under different concentrations and molar ratios of the two peptides. For the solutions containing Ac–A₆D–OH only, nanorods became transformed into chiral nanoropes with increasing solution concentration. The nanoropes were formed by assembling numerous nanorods and the left-handedness was caused by the inherent twisting (image inserted in Fig. 5B). For solutions containing Ac–A₆K–NH₂ peptide only, increase in peptide concentration resulted in the structural transformation from spherical

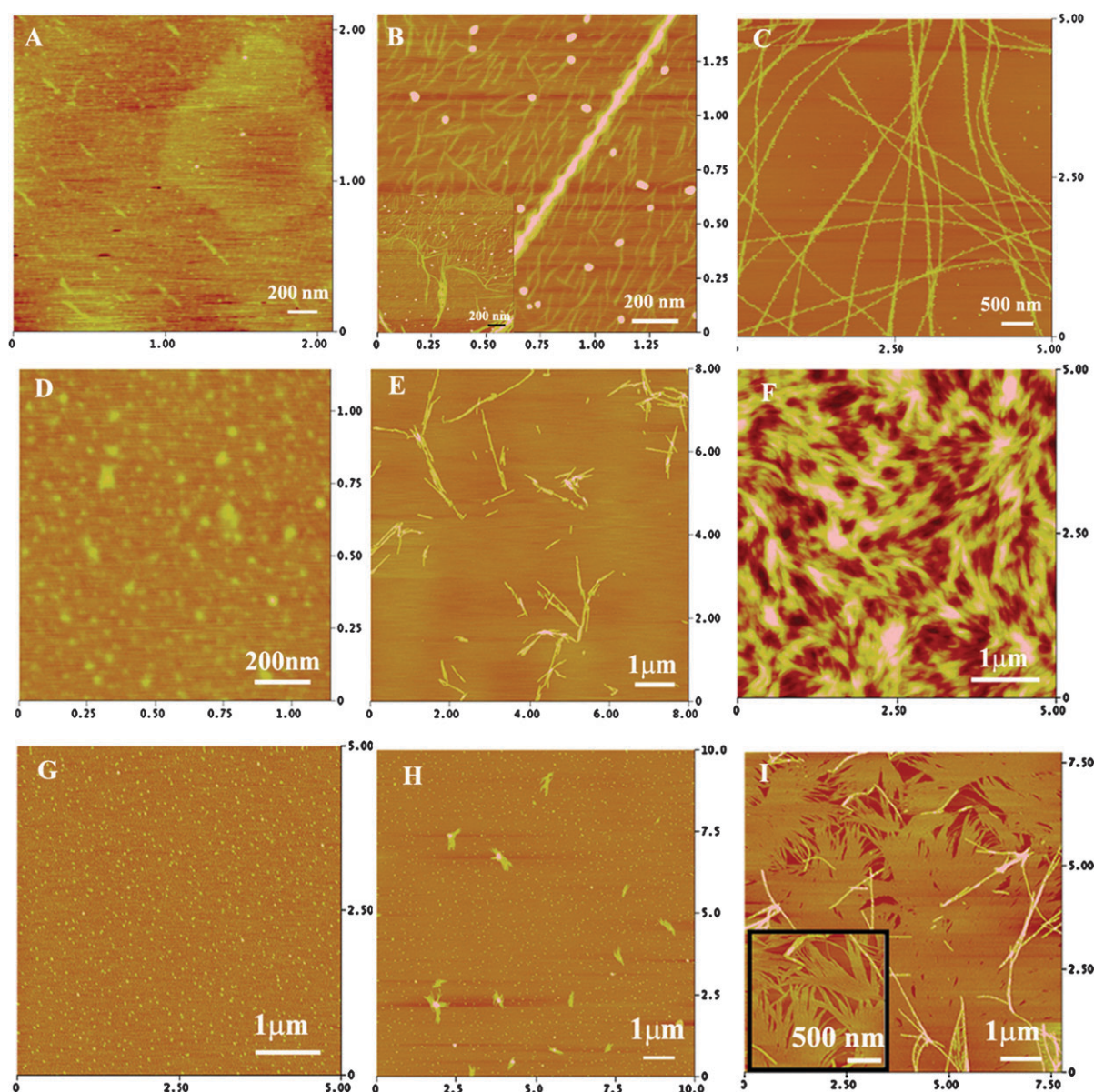


Fig. 5 Synergistic effects of designer peptides illustrated by the AFM images of Ac-A₆D-OH, Ac-A₆K-NH₂, and their mixture on freshly cleaved mica surface under ambient conditions. AFM images for the nanorod and nanorope structures of Ac-A₆D-OH with the concentrations of 1 μM (A), 70 μM (B), and 1 mM (C). The inset in B illustrates the intermediate state for the twisting of nanofibers to form the helical nanoropes. (D), (E) and (F) illustrate AFM images for the nanorod structures of Ac-A₆K-NH₂ at the concentrations of 1 μM, 70 μM, and 1 mM, respectively. The AFM images for the nanofilm structures consisted of nanoropes for mixed peptides Ac-A₆D-OH/Ac-A₆K-NH₂ (G, H, and I) with the concentrations of 1.5 μM (G), 15 μM (H), and 1.5 mM (I). The concentrations of the total peptides were used for the mixture solutions. The molar ratios for the solutions were Ac-A₆D-OH/Ac-A₆K-NH₂ = 2 : 1 and the inset in (I) is the high-resolution image showing the nanorope structure at domain boundaries. (Reproduced from *Nano Today* 2009, 4, 193. Copyright © 2009 Elsevier Ltd.).

nanoparticles to rigid nanorods, then to the stacking of nanorods (Fig. 5D–F). Mixing of the two peptides at the molar ratio of unity led to the formation of uniform nanoropes. It is thought that the two peptides are randomly oriented and distributed as monomers in solution at concentrations well below the CAC. The interdigitated short and thin nanorods, or spherical particles were formed due to the electrostatic attraction between opposite charges and the hydrophobic interactions between alanine tails. They then arranged themselves alternatively to reduce the energy. Nanoropes could be formed by the extension of the spherical

particles or self-assembled stacks at high concentrations. Thin films could also be formed by fine-tuning of the charges and the hydrophobicity of the peptides. These observations are valuable for understanding peptide self-assembly behaviour in mixed systems and for technological applications.

Synergistic effects were also observed at different interfaces when examining the co-adsorption of Ac-V₆K-NH₂ peptide and conventional surfactants SDS (anionic) or C₁₂TAB (cationic). The peptide alone achieved the adsorption plateau at the hydrophilic SiO₂/water interface with the adsorbed amount at 3.2 mg m⁻² within 10 min. The adsorption

proceeded very fast at the early stage and subsequently became very stable against time. However, the peptide behaved differently in the presence of different amount of SDS. At the molar ratio of 0.5:1 (SDS/V₆K), the adsorption reached the same plateau as the pure peptide but the process was slower, showing the impact of charge neutralization and the weakening of the driving force. When the ratio increased to 0.78:1, the adsorption dynamic process was slowed down further with lower adsorbed amount. However, when the molar ratio further increased to unity or above, only a negligible amount (less than 0.2 mg m⁻²) of adsorption was detected. This observation indicated that the adsorption of the peptide could be inhibited by the presence of SDS and that the driving force was electrostatically based at this interface. As the molar ratio was equal to the charge ratio, SDS interacted with the peptide mainly through electrostatic interaction. When the molar ratio was below unity, SDS was not enough to neutralize all the peptide molecules in solution, thus excess peptides contributed to surface adsorption. Therefore, both of the adsorbed amount and dynamic process were slowed down as the molar fraction of SDS went up at the weakly charged substrate surface. However, at this moment, it is not clear whether hydrophobic interaction had any role to play. Further experiments using neutron reflection will help identify the composition of surfactant and peptide at the interface and thus provide useful information about how to tune the surfactant-peptide interaction through hydrophobic affinity.

To further assess the effect of electrostatic interaction, coadsorption with cationic C₁₂TAB was also studied. It was found that the adsorption of C₁₂TAB and V₆K at the ratio of 1:1 was very similar to that of the pure peptide except the slightly lower adsorbed amount. This might indicate that the adsorption was mainly contributed by the peptide. But the existence of C₁₂TAB reduced peptide adsorption. When the ratio increased to 20:1, the final plateau surface adsorbed amount was further reduced. The dynamic process of adsorption was also dramatically slowed down. This was attributed to the competitive adsorption between C₁₂TAB and V₆K as they were both cationically charged. Further increase in the ratio to 94:1 resulted in a significant drop of surface adsorption. At this stage the C₁₂TAB reached its CMC and was in high excess. Thus C₁₂TAB dominated the adsorption.

3.2 Lipopeptides

An example of natural lipopeptides is surfactin, a cyclic lipopeptide produced by the Gram-positive bacteria *Bacillus subtilis*. Its CAC is dependent on acyl chain branching and mixing and is also sensitive to temperature. It can disrupt bacterial membrane structures and thus has excellent antimicrobial activity.¹⁰⁴ Inspired from Nature, many designed lipopeptides have also been synthesised for different applications. A common feature of lipopeptides is that an acyl carbon chain is linked to the N terminal of a peptide sequence. A simple example of this is C_mK_n, while *m* is the length of acyl tail and *n* is the number of lysine residues in the peptide head group.

Extensive studies have recently reported that lipopeptides could self-assemble to form interesting nanostructures. Taking

C₁₆-W3K (C₁₆H₃₁-WA₄KA₄KA₄KA) as an example, the C₁₆ acyl chain was linked to the W3K peptide sequence which formed α -helix with the charged groups symmetrically distributed around the helical structure. The self-assembly of the C₁₆-W3K molecules was found to be a slow dynamic process. It formed spherical micelles with diameters around 10 nm, which then gradually transformed into worm-like micelles after days. Concurrently, the secondary structure of the head groups gradually transformed into a β -sheet conformation and the molecules eventually formed long nanofibers after 13 days.⁵⁷ Apart from the nanofibrillar structure, nanobelt and nanoribbon structures have also been reported by the self-assembly of C₁₆H₃₁-O-VEVE lipopeptide.⁵⁸ The head group of this lipopeptide contains both hydrophilic (E, negatively charged) and hydrophobic (V) residues, with E residues on one side of the molecule and V residues on the other side (Fig. 6A). The long nanobelts were formed after two days with heights between 10–20 nm and widths around 150 nm (Fig. 6B–D) and with the β -sheet conformation becoming dominant in the nanobelts. The nanostructures formed by this lipopeptide were also concentration dependant and reversible. Narrower nanobelts and twisted nanoribbons were observed at low concentrations. As concentrations increased nanobelts became dominant (Fig. 6E and F). Meanwhile, the flat nanobelts could transform into “grooved” nanobelts with increasing solution pH due to the increasing repulsion between the partially deprotonated glutamate residues. This process was reversible as well when the acidic pH was returned. Similar work has been reported by Deng *et al.*⁵² using an amyloid β -peptide (EVHHQKL) connected with a C₁₂ acyl chain at the N-terminal (C₁₂-A β (11–17)). Rod-like nanofibrils with diameters around 5 nm and variable lengths could be formed through self-assembly at around pH 3. Increased concentrations resulted in the parallel packing of the nanofibrils through lateral association. At the basic pH around 10, twisted nanobelts were observed. Under these conditions, formation of the β -sheet structure by the head groups was dominant. Other pH responsive lipopeptides (such as C₁₀-A₄G₃S^(PO₄)RGD and C₁₆-C₄G₃S^(PO₄)RGD) have also been reported.⁵³ These molecules self-assembled into nanofiber networks at low pH and disassembled into a fully dissolved state with increasing pH.

Apart from solution pH, other environmental conditions such as salt addition⁵⁹ and light illumination¹⁰⁵ have also been demonstrated to affect lipopeptide self-assembly strongly. The addition of salt resulted in different mechanical properties of self-assembled nanofibrillar gels. It was found that calcium-mediated ionic bridges in CaCl₂-lipopeptide (C₁₆-V₃A₃E₃) gels formed stronger intra- and inter-fiber crosslinks than the hydrogen bonds formed by the protonated carboxylic acid residues in HCl-lipopeptide gels.⁵⁹ Therefore, the calcium gels could withstand higher strains than the normal hydrogen bond gels. However, the latter was easier to recover after sustained deformation at 100% strain. The solution of a lipopeptide containing a photo-cleavable 2-nitrobenzyl group remained clear under self-assembling conditions. However, the solution became gelled after photo-irradiation at 350 nm.¹⁰⁶ TEM revealed a steady transition from spherical structure into cylindrical nanostructure after photo-irradiation. Cell culture on the light-triggered lipopeptide suggested increased

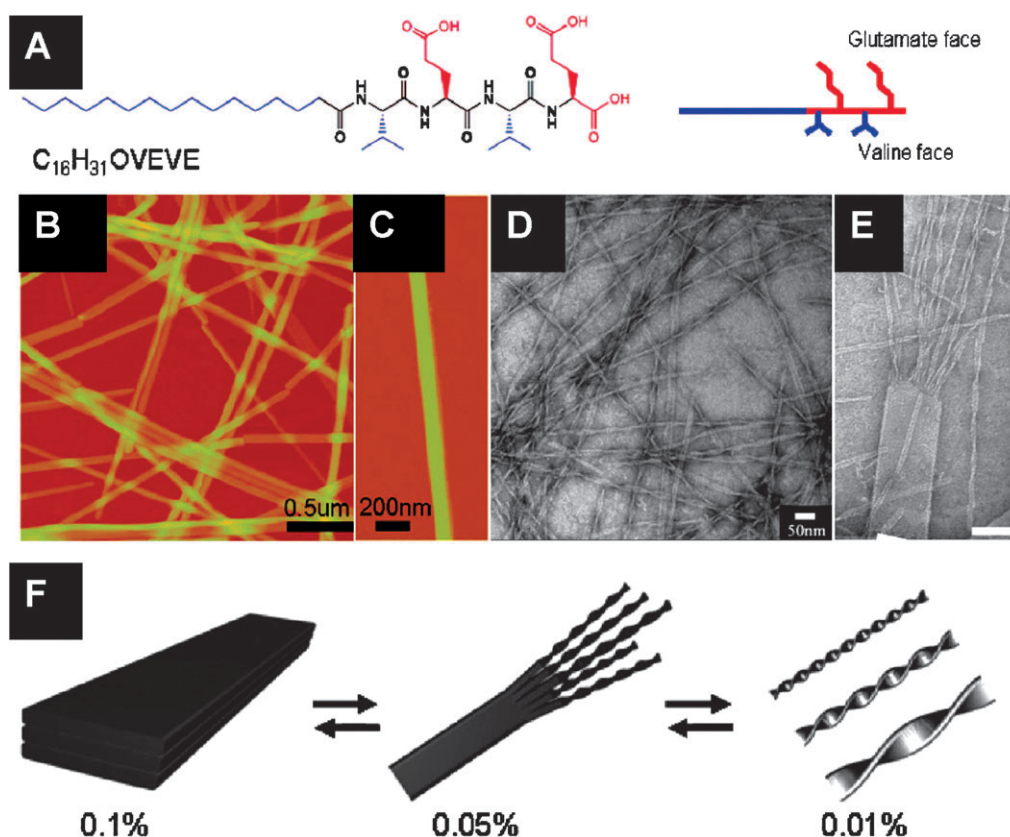


Fig. 6 Giant (ultra-long and wide) nanobelts assembled from a peptide amphiphile containing four amino acids and an acyl tail. A, chemical structure of the peptide amphiphile. B and C, AFM images of peptide nanobelts at different scanning sizes. The assembled nanobelts are the dominant structures in the assembly system. D, narrower nanobelts and twisted nanoribbons are observed at a concentration of 0.01 wt%. The twist pitch changes with nanoribbon width. E, twisted nanoribbons sprouting from one nanobelt end. F, schematic representations of the morphological transitions with lipopeptide concentration. Scale bars of panel F: 100 nm. All the TEM samples were negatively stained with 2% (w/v) uranyl acetate aqueous solution. (Adapted from *Nano Letters*, 2009, 9, 945. Copyright © 2009 American Chemical Society.)

bioactivity.¹⁰⁷ By modifying the peptide sequences, different rates of gelation kinetics were achieved without disturbing the biofunctional segment.¹⁰⁸ It was found that the pre-existence of hydrogen-bonded aggregates in the solution state of more hydrophobic peptide amphiphiles accelerated gelation while modification of the sequence into more hydrophilic and bulky amino acids suppressed the formation of the nanostructures and gels, and effectively slowed down the self-assembly of the nanofiber network. Modification of gelation kinetics without disrupting bioactivity could be important to *in vivo* applications in regenerative medicine.

3.3 Biomimetic peptide amphiphiles

Certain biomimetic peptide sequences derived from key proteins have the potential as therapeutic agents for treating many diseases.⁶³ However, they have difficulties to cross the cell membranes to reach the target position. Different cell-penetrating peptides (CPPs) have been incorporated with them to help their internalization. A simple alternative is to attach a hydrophobic tail to the peptide sequence making the molecule amphiphilic. These peptide amphiphiles have good affinity to cell membranes as the hydrophobic tails can insert into the membrane lipids and improve the transportation through cell membrane.⁶³ The 16-mer peptide

(LSQETFSDLWKLLPEN) that can inhibit the p53-MDM2 protein interaction has been linked to a C₁₆ acyl tail. Improved internalisation into the SJSA-1 human osteosarcoma cell line has been reported using this biomimetic peptide amphiphile. Biomimetic peptide C₁₆-GTAGLIGQERGDS-COOH contains not only a proteolytically degradable sequence GTAGLIGQ, where cleavage occurs between glycine and leucine, but also a cell-adhesion sequence RGDS.⁶⁴ The addition of calcium ions leads to the self-assembly of the molecules into long nanofibers. Cell growth results on the nanofiber networks have demonstrated that the biomimetic peptides had better performance in cell adhesion compared with the ones without RGDS. The presence of RGDS enhanced the expression of MMP2 enzymes, which could degrade the GTAGLIGQ sequence, thereby facilitating cell migration and proliferation.

4. Applications of peptide amphiphiles

4.1 Antimicrobial activities

There is an increasing demand to develop new antimicrobial agents due to the increasing resistance of microbes against conventional antibiotics. Short designed cationic peptides are potential candidates as future antimicrobial agents. Unlike the

traditional antibiotics, which normally work as bacterial growth inhibitors, cationic antimicrobial peptides kill the microbes by interacting and disrupting bacterial cell membranes. Both cationic charges and hydrophobicity play vital roles in the effectiveness of microbial killing. Whilst the lengths of most antimicrobial peptides vary from 10 amino acid residues to a few dozen residues, the designed ones are normally 6 to 15 residues in length. The designed sequences, amphiphilic or biomimetic, are mostly rich in certain amino acids such as K, R, D and E as hydrophilic moiety and hydrophobic residues such as A, V, I, L, F, W and Y as hydrophobic moiety. The portion of hydrophobic residues is usually greater than the charged one, but if the hydrophobic residues are large such as I, L and W, the portion of the hydrophobic residues may go down. Some antimicrobial peptides also contain repeat sequences and readily form α -helices, relaxed coils and antiparallel β -sheets in solution

or under membrane environment. After adopting the stable secondary structures, these antimicrobial peptides often display characteristic amphipathicity.^{109,110} These structural features allow them to attach to and insert into microbial membrane bilayers to form pores by ‘barrel-stave’, ‘carpet’ or ‘worm-pore’ mechanisms and eventually disrupt the cell membranes.^{109,111} As already indicated, designed amphiphilic ones have relatively simple molecular structure. The head group is usually composed of a few K, R or H that bear cationic charges at biological pH whilst the hydrophobic chain can be either acyl chain or a few non-polar amino acid residues as listed above.

Peptide amphiphiles A_mK ($m = 3, 6$ or 9) displayed a varying extent of antimicrobial activities, supported by evident permeation and disruption to the bacterial membranes (Fig. 7A).²⁰ As the length of peptide hydrophobic tail increased, the extent of membrane penetration and the ability

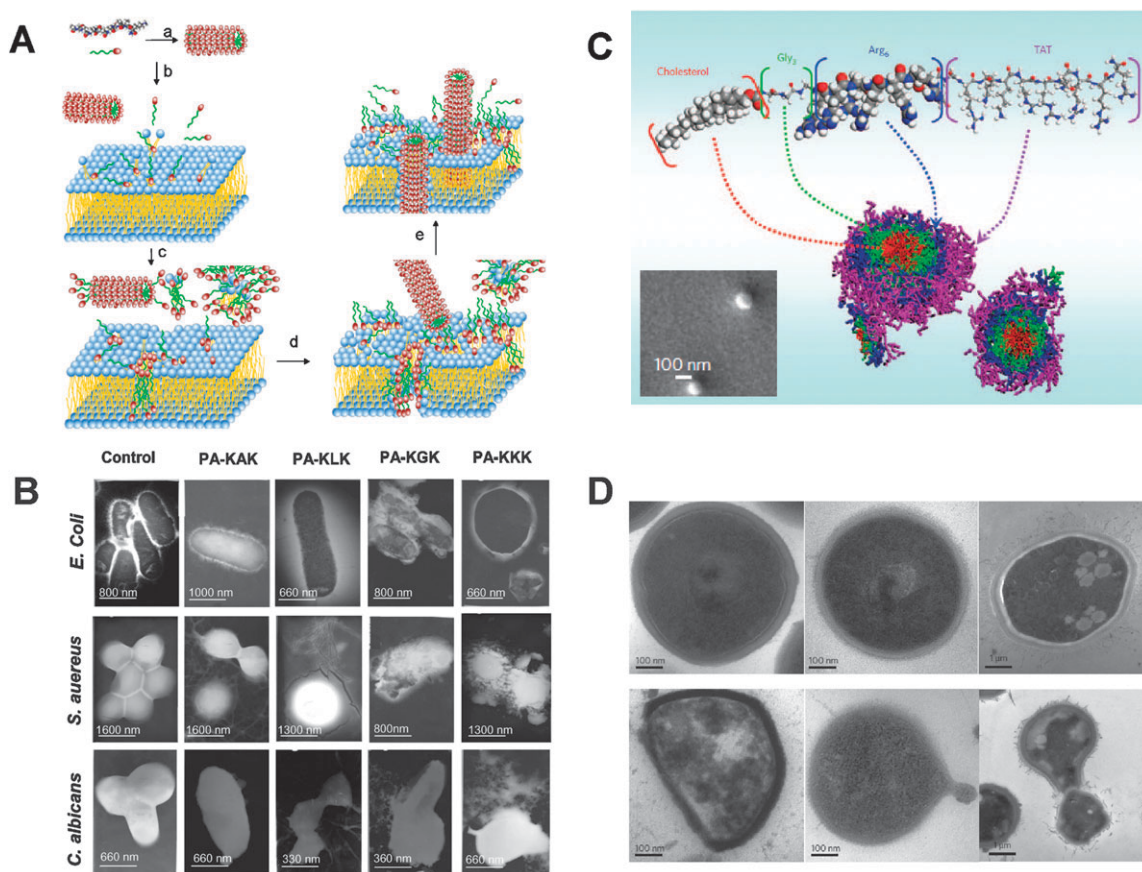


Fig. 7 A, Schematic illustration of mechanisms of action adopted by A_9K for the bacterial membrane permeation and disruption. The red rods represent A_9K nanorods. The A_9K molecules assemble into nanorods with the positive charges outside (step a). The monomers may also flap out and become inserted into the outer membrane surface (step b). They can then flip and become inserted into the inner leaf of the membrane, forming a “through barrel” or micelle to cause leakage or lysis (step c). Nanorods formed may also attack cell membrane through electrostatic attraction or local hydrophobic affinity, lifting some lipids out of the membrane and making the membrane unstable, causing the nanorods to flop into the membrane bilayer (step d and e). B, Electron micrographs of negatively stained *E. coli* (top), *S. aureus* (middle), and *C. albicans* (bottom) untreated or treated with the C_{16} -KXX series of lipopeptides. The lipopeptides were used at their MICs. C, Molecular cartoon of Chol- G_3R_6 TAT and formation of micelles, simulated through molecular modelling using Materials Studio software. (SEM image of nanoparticles inserted). D, TEM images of *S. aureus*, *E. faecalis*, and *C. neoformans* before (up row) and after (bottom row) incubation with 32 mM of nanoparticles for 2 h. (A was reproduced from *Biomacromolecules* 2010, **11**, 402. Copyright © 2010 American Chemical Society. B was reproduced from *Biochemistry* 2008, **47**, 10630. Copyright © 2008 American Chemical Society. C and D were adapted from *Nature Nanotechnology* 2009, **4**, 457. Copyright © 2009 Macmillan Publishers Limited.)

to cause bacterial aggregation and clustering increased. For A₉K, the power for membrane permeation and bacterial clustering intensified with peptide concentration and incubation time. The results depicted a positive correlation between the propensity for self-assembly of the peptides, their membrane penetration power and antimicrobial capacity. Like natural antimicrobial peptides, A₉K killed bacteria also *via* permeating cell membranes. The membrane permeability and cell lysis induced by A₉K have been observed with fluorescent assay and SEM characterisation and the results showed a consistent trend of dependence on peptide concentration and incubation time. A₉K exhibited the best killing capacity against Gram-negative and Gram-positive bacteria among the peptide series studied.

Lipopeptides have also been designed and investigated for their antimicrobial effectiveness. Mitra *et al.*¹⁹ studied lipopeptide-based molecules with proline (P), phenylalanine (F) or tryptophan (W) as part of the head groups and C₁₄ as tails. These lipopeptides showed remarkable growth inhibition activity on both Gram-positive and Gram-negative bacteria and fungus. In addition, they have good biocompatibility to different mammalian cell lines like HepG2, HeLa and SiHa. Similar capability was observed from their C₁₆ analogues.¹⁹ C₁₆-KXX series of lipopeptides (X designates A, G, L, or K) have also been reported to be potent to both bacteria and fungi.⁶² Interestingly, C₁₆-K and C₁₆-KAK were rather inactive while C₁₆-KLLK only active to Gram-positive bacteria and fungi. C₁₆-KK, C₁₆-KKK and C₁₆-KGK, however, showed powerful activities to both Gram-positive and negative bacteria and fungi as well (Fig. 7B). Among the lipopeptides they studied, C₁₆-KKK is the best antimicrobial lipopeptide.

Recently, the membrane translocation sequence TAT (YGRKKRRQRRR) found from the transcriptional activator TAT protein of the human immunodeficiency virus type-1 (HIV-1) has been used to construct the antimicrobial agent.⁶⁶ The molecule (Chol-G₃R₆TAT) contains a hydrophobic tail of cholesterol which helps the self-assembly, three glycine residues as spacer, six arginine residues to enhance the performance of membrane translocation sequence TAT (Fig. 7C). Core-shell structured micelles were predicted to form by the peptide with the cholesterol inside as hydrophobic core and cationic peptide outside as hydrophilic shell. The peptide had a CAC of 10 μM in deionized water. The formation of micelles resulted in an increased cationic charge density at the outside of the nanoparticles, therefore enhancing the antimicrobial activity. The presence of the TAT sequence could also help the nanoparticles to cross the blood-brain barrier (BBB) to the brain, hereby making the molecule a good candidate for the brain infection treatment. The hydrodynamic diameter, gyration of diameter, aggregation number and zeta potential of the micellar particles were estimated to be 177 ± 6 nm, 152 ± 8 nm, 91 and 55 ± 4 mV, respectively. The nanoparticles showed strong antimicrobial effects against drug-resistant bacteria, yeast and fungi. SEM results revealed the disruption and lysis of cell walls of both bacteria and fungi (Fig. 7D). The performance was even better than conventional antibiotics penicillin G and doxycycline in killing *B. subtilis* and

antifungal agents fluconazole and amphotericin B in inhibiting the proliferation of *S. chartarum*. *In vivo* experiments demonstrated that the peptide nanoparticles had high therapeutic index against *S. aureus* infection in mouse model and could penetrate the BBB and suppress bacterial growth in the brain using a rabbit model.

4.2 Cell culture scaffold for tissue engineering

The attractive features of nanostructures associated with gel network formation and antimicrobial effects from peptide amphiphiles make them ideal candidates as cell culture matrixes or scaffolds in tissue engineering and regenerative medicine. Extensive studies have already indicated their good biocompatibility.¹¹² A simple peptide Fmoc-RGD mimicking the extracellular matrix (ECM) has recently been reported, where Fmoc as a hydrophobic moiety was linked to the tri-peptide sequence RGD forming an elegant peptide amphiphile. These molecules self-assembled into nanofibers and bioactive hydrogels through π-π stacking of the Fmoc groups, leaving the RGD groups outside the nanofiber surfaces. The self-assembled hydrogels displayed excellent performance in 3D cell culture using human adult dermal fibroblast cells.¹¹ Peptide amphiphiles have also been used to create 3D micro-scale topographical patterns to study the behaviour of human mesenchymal stem cells (hMSCs).⁶⁷ The hydrophilic part of the amphiphile was a peptide sequence RGDSKLLA(K) containing the cell adhesive epitope RGD while the hydrophobic tail was alkyl chain (-C₈H₁₆-diacetylene-C₁₂H₂₅) bearing a photosensitive group diacetylene which could covalently link the self-assembled molecules upon UV irradiation. Well-defined nanofibers could be formed through self-assembly of these kind of peptide molecules. Pattern fabrication was started by applying the PDMS mould to the freshly dissolved or aged peptide solutions on a silica substrate. The self-assembly and polymerisation of the peptide gel were then achieved by exposure to ammonium hydroxide followed by UV irradiation. Cell growth on the patterned peptide amphiphile surfaces demonstrated that cells not only recognised the biomolecular signalling provided by RGDS epitopes but also the physical guidance provided by the topographical patterns (Fig. 8).⁶⁷ In addition, the authors found that cell differentiation was significantly affected by the type of substrate created. Enhanced differentiation was found on the material surfaces containing RGDS. Hole micro-textures were better for the osteoblast differentiation than all other surfaces. The negatively charged C₁₆-V₃A₃E₃ peptide coated surface was demonstrated to be suitable for the growth of bone-marrow mononuclear cells (BMNCs). In addition, a binary peptide system containing 10 wt% C₁₆-V₃A₃K₃RGDS and 90 wt% C₁₆-V₃A₃E₃ lipopeptide molecules was found to promote optimal cell adhesion.⁶⁰ *In vivo* delivery of luciferase-expressing cells using the binary lipopeptide nanofiber system into the mouse model revealed the enhanced viability and proliferation of associated bone marrow derived stem and progenitor cells. Lipopeptides with branched head groups containing RGDS also showed excellent performance as scaffolds for the growth of human bladder smooth muscle cells.⁶¹

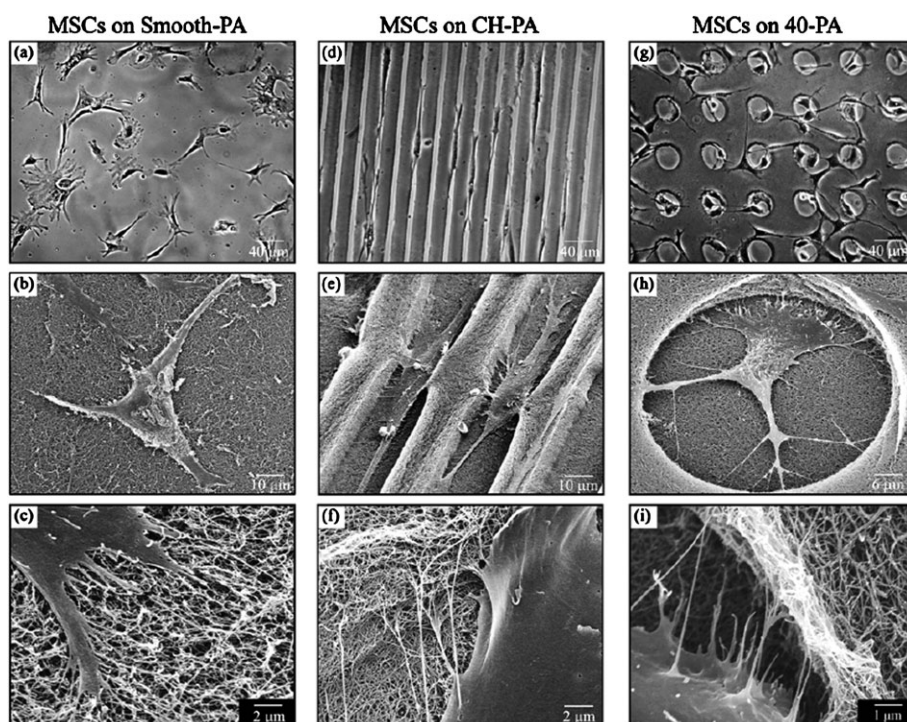


Fig. 8 Morphological characteristics of cells on various peptide amphiphile (PA) substrates. (a–c) Cells on smooth peptide amphiphile exhibited broad flattened shape with randomly oriented processes. (d–f) In contrast, hMSCs on CH-PA (10 μm wide channels separated by 20 μm distances) exhibited narrower cell bodies that aligned along the microchannel axis while (g–i) those growing on 40-PA (surfaces with 8 μm deep holes that were 40 μm in diameter, and 8 μm high) tended to migrate and spread inside the 40 μm diameter holes. On all substrates, hMSCs interacted with the PA nanofiber bundles (c, f, i), which were especially evident along the vertical geometries of the channels (f) and holes (i). (Reprinted from *Soft Matter*, 2009, 5, 1228. Copyright © 2009 The Royal Society of Chemistry.)

4.3 Skin care and cosmetics

Surfactants have been widely used in personal care products such as shampoos and cosmetics. The main roles of traditional surfactants such as sodium dodecyl sulfate, sodium myreth sulfate are cleaning and foaming. In contrast, peptide amphiphiles can not only act as surfactants, but they also have inherent biological functions such as *anti-wrinkle*, antimicrobial activities, and can be directly used as nutrients. They therefore have great potential for cosmetic applications.¹¹³ Palmitoyl pentapeptide-3 or 4 (Matrixyl) is a typical lipopeptide with a C_{16} acyl chain as tail and a peptide sequence KTTKS as head. The short peptide is a structural mimic of part of the sequence of collagen type I. The attachment of the fatty acid tail clearly enhances its oil solubility and improves skin penetration. The peptide sequence, when used in the culture of fibroblast cells, stimulates the synthesis of the key constituents of the skin matrix such as collagen, elastin and glucosaminoglycans. Although the exact mechanism is not well understood, the lipopeptide has been used in a variety of *anti-aging* products and has exhibited effectiveness against wrinkles with no skin irritation.⁶⁸ A peptide fragment derived from immunoglobulin G has also been incorporated with palmitic acid to make the lipopeptide called palmitoyl tetrapeptide-3 or 7 (C_{16} -GQPR). It is one of the important active ingredients in Matrixyl™ 3000. Ageing and UV radiation cause the elevated level of expression of interleukins, which triggers inflammation. Palmitoyl tetrapeptide-3 or

7 molecules are thought to help suppress the expression of interleukins, thereby reducing inflammation. Palmitoyl oligopeptide such as C_{16} -GHK is another important active ingredient in Matrixyl™ 3000. The GHK sequence is also a fragment of type I collagen. The degradation of the skin matrix results in the increased level of the GHK short sequence, which serves as a signal feedback for fibroblast cells to synthesize new skin matrix. The addition of C_{16} -GHK can presumably stimulate skin matrix replenishment and reduce wrinkles.⁶⁹

4.4 Drug and gene delivery

Peptide amphiphiles are excellent candidates for drug delivery due to their *trans*-membrane capability. The amphiphilic nature of peptide molecules and self-assembled nanostructures can facilitate the internalisation of the drugs encapsulated by them. A number of cationic peptide amphiphiles have been reported as drug and gene delivery carriers. Self-assembled cholesterol-conjugated H_5R_{10} and $\text{H}_{10}\text{R}_{10}$ oligopeptides outperformed PEI in plasmid DNA delivery into both HepG2 and HEK293 cell lines. Increasing the number of histidine residues was found to further enhance gene expression efficiency.⁴⁸ It was thought that weak cationically charged histidine served as “proton sponge” and could enhance gene delivery. Peptide amphiphiles with different tails ($\text{NH}_2\text{-I}_5^-$, $\text{NH}_2\text{-W}_5^-$, $\text{NH}_2\text{-F}_5^-$) but with the same head group ($\text{-H}_4\text{R}_8\text{-CONH}_2$) have been compared for their gene delivery capability. Different gene expression efficiencies were

observed, indicating the impact of tail hydrophobicity.⁴⁷ Peptide amphiphiles A₁₂H₅K₁₀ and homologues have shown comparable gene delivery efficiencies to PEI but with better biocompatibility. These peptides, when dissolved in aqueous solution, would form core-shell structured nano-assemblies with diameters around 800 ± 100 nm, CACs around 1 mg ml⁻¹, and zeta potentials around 19 mV. The authors proposed that charge mediated interaction occurred *via* the cationically charged micelles and DNA. It was thought that the increased cationic charge density at the outside of the micellar shell offered better DNA binding capability and protected the DNA from enzymatic degradation. However, because free peptide amphiphile molecules were also present in the solution, complexation with DNA might also proceed through direct molecular interaction. The molecular complexation might produce smaller complexes in greater numbers and might affect the entire transfection efficiency more significantly. Results have also shown that the addition of A₁₂ tail to H₅K₁₀ improved the gene expression without causing significant increase in cytotoxicity.⁵⁰ However, due to the weak hydrophobicity of the A₁₂ tails, these peptides were not effective at delivering hydrophobic drugs such as doxorubicin and paclitaxel.⁴⁹ To increase the hydrophobicity of the tails, six alanine residues inside the tail have been replaced by phenylalanine residues. The new cationic peptide amphiphile Ac-(AF)₆-H₅-K₁₅-NH₂ has been evaluated as carrier for co-delivery of drug (doxorubicin) and genes (luciferase reporter gene and p53 gene).⁴⁹ The peptide self-assembled into similar cationic core-shell nanostructures with CAC, size and zeta potential at 0.042 mg ml⁻¹, 102 ± 19 nm and 22.8 ± 0.2 mV, respectively. Increasing hydrophobicity in the tail resulted in CMC reduction but increased zeta potential. The nanostructures could then efficiently encapsulate doxorubicin into the micelles and achieve sustained release without obvious initial burst. Compared with the free doxorubicin, micelles loaded with doxorubicin had better internalisation capability into the HepG2 cells (Fig. 9A). Simultaneous delivery of a model drug (hydrophobic FITC) and gene (rhodamine-labelled DNA) have also been achieved (Fig. 9B). The co-delivery of doxorubicin and p53-encoding plasmid using the self-assembled nano-micelles synergistically suppressed the proliferation of HepG2 cells.⁴⁹ Therefore, designed peptide amphiphiles have great potential as effective carriers for both drugs and genes for therapeutic applications.

4.5 Templates for nanofabrication and biomimetalisation

Self-assembling peptide amphiphiles have great potential as templates for nanofabrication such as biomimetalisation, nucleation, nanowires, nanocircuits.¹¹⁴ In 2001, a lipopeptide was designed and synthesized for biomimetalisation by the Stupp group.⁵⁴ The C₁₆ tail was connected to the N terminal of a peptide sequence which contained four cysteines, three glycines, a single phosphorylated serine and a cell adhesion ligand RGD (C₁₆-C₄G₃S^(P)RGD-OH) (Fig. 10A). The connection of the C₁₆ tail made the molecule amphiphilic and facilitated the self-assembly in aqueous phase into cylindrical micellar structure. C₁₆ acyl tails packed themselves in the centre of the micelle as the hydrophobic core with the

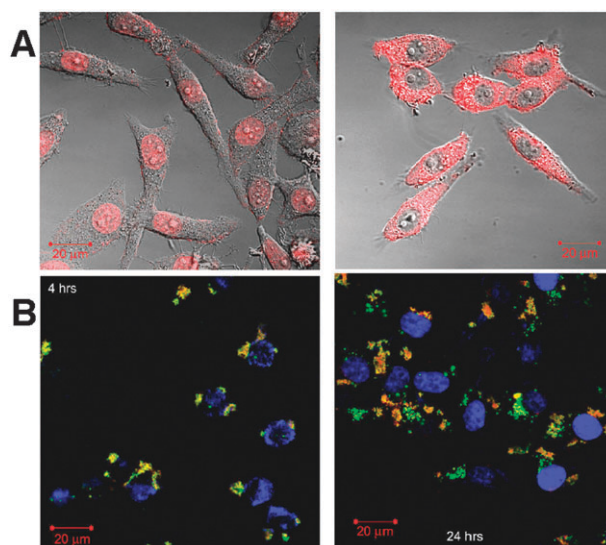


Fig. 9 A, confocal images of HepG2 cells treated with free doxorubicin (left) and doxorubicin-loaded FA32 (right). Doxorubicin concentration: 1 mg L⁻¹. B, confocal images of HepG2 cells treated with FITC-loaded FA32 micelle/rhodamine-labelled DNA complexes formed at N/P = 18 for 4 h. Left: cells imaged right after 4 h transfection; Right: cells observed after another 20 h incubation post-transfection. (Reproduced from *Biomaterials* 2009, **30**, 3100. Copyright © 2009 Elsevier Ltd.)

hydrophilic peptide sequences forming β -sheets at the outside.¹¹⁵ The intermolecular disulfide bonds formed by the cross-linking of the 4-cysteine residues in the middle of the molecules made the self-assembled nanofibers robust and impervious to pH variation. The nanofibers were then used to direct the mineralisation of hydroxyapatite.⁵⁴ The hydroxyapatite nucleated on the surfaces of the lipopeptide nanofibers and its crystals grew with their C axes oriented along the long axes of the nanofibers. This alignment was the same as that observed between collagen fibers and hydroxyapatite crystals in bone. Reported by the same group, self-assembled lipopeptide nanofibers have been used as bioactive materials to coat the bone implant materials consisting of a Ti-6Al-4V foam (Fig. 10C).¹¹⁶ Results demonstrated that the nanofiber matrices occupied the pores of the metallic foam and that cells were encapsulated within the bioactive matrices. Meanwhile, the nanofibers could also facilitate the mineralisation of hydroxyapatite. The inert titanium covered by the nanofiber matrix was transplanted into Sprague Dawley rat model. Bone formation was observed around and inside the implant, and vascularisation was also observed around the implant with the absence of a cytotoxic response. 3D bone-matrix mineralisation using similar lipopeptides as templates has also been reported recently.¹¹⁷

Meanwhile, the nanofibers have also been used as templates for the nucleation and growth of CdS nanocrystals (Fig. 10D).¹¹⁸ The presence of Cd²⁺ in solution resulted in the supersaturation of the ions around the nanofibers. Nanostructured CdS crystals were formed when hydrogen sulfide (H₂S) was diffused into the system. Hollow silica nanotubes with tunable dimensions have also been achieved on the C₁₆-A₄K₄ peptide nanofiber templates followed by

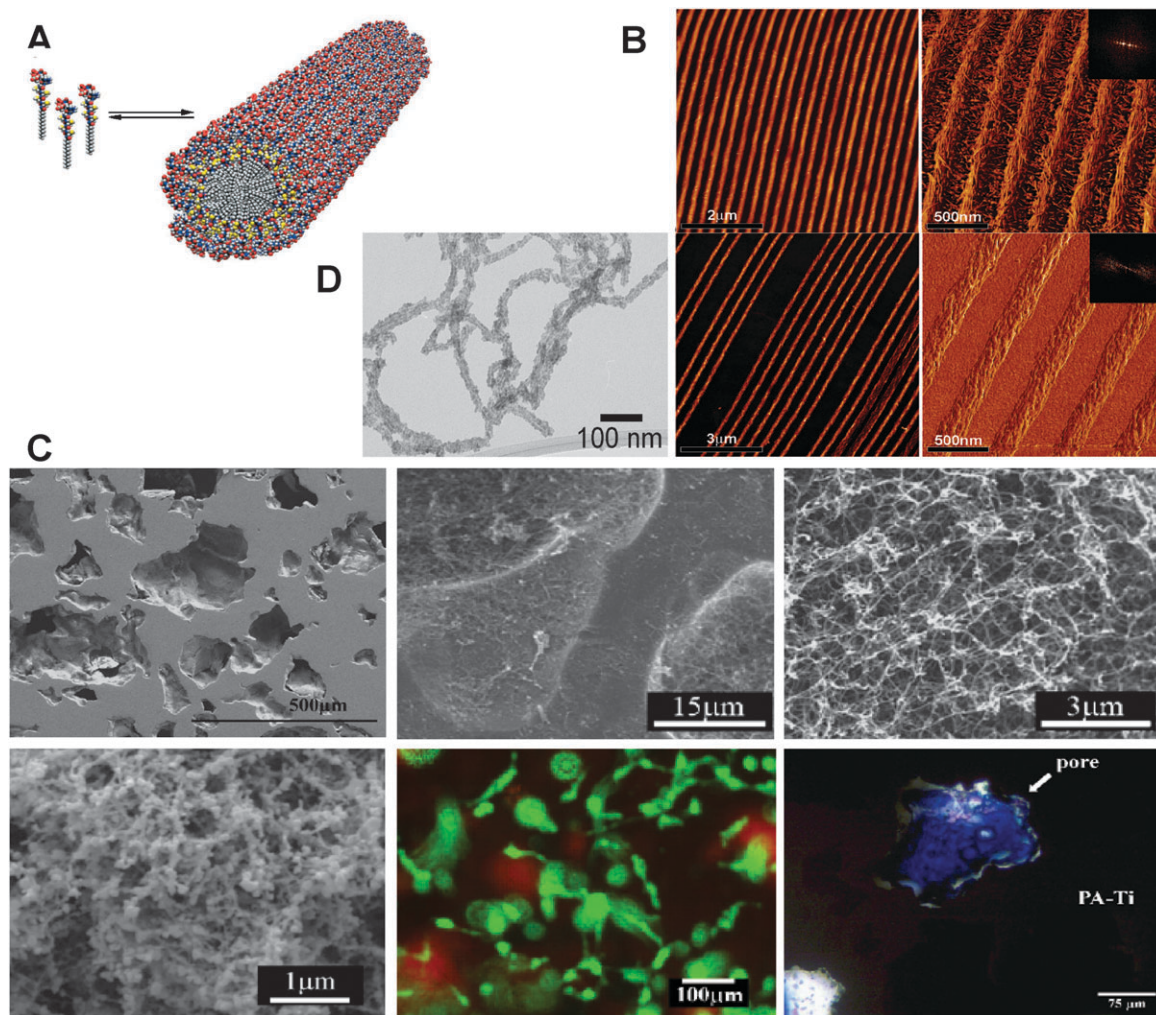


Fig. 10 A, schematic model of the self-assembly of peptide amphiphiles into a cylindrical micelle. The molecule (shown as the last in Fig. 1) contains five key structural features: a long acyl tail that conveys hydrophobic character to the molecule and, when combined with the peptide region, makes the molecule amphiphilic; four consecutive cysteine residues that when oxidized may form disulfide bonds to polymerize the self-assembled structure; a flexible linker region of three glycine residues provides the hydrophilic head group flexibility from the more rigid cross-linked region; a single phosphorylated serine residue that is designed to interact strongly with calcium ions and that helps direct mineralisation of hydroxyapatite; the cell adhesion ligand RGD. B, AFM height and phase images of aligned supramolecular nanofibers of $C_{16}\text{-A}_4\text{G}_3\text{S}^{(P)}\text{RGD-COOH}$ (Top) and $C_{16}\text{-A}_4\text{G}_3\text{EIKVAV-COOH}$ (Bottom). The fibers were embossed from 5 wt% and 1 wt% solutions into lines with periods of 278 nm and 417 nm (height scales 99.8 nm and 44.7 nm, respectively). The widths were all around 150 nm, and the average heights of the lines were around 33 nm and 24 nm, respectively. C, Top left, SEM micrograph of polished, bare Ti-6Al-4V foam in cross-section; Top middle, higher magnification of the peptide amphiphile coating on the Ti-6Al-4V foam surface and filling the pores; Top right, higher magnification of the self-assembled peptide amphiphile nanofibers forming a 3D matrix within the pores; Bottom left, mineral formation only on the nanofiber indicating templation on the nanofibers; Bottom middle, microscopic image of the green fluorescence from the live cells encapsulated within the nanofiber matrix of the peptide amphiphile; Bottom right, mineralized bone formation (blue) within an interior pore of the peptide-Ti-6Al-4V hybrid. D, Bright field TEM micrographs of CdS mineralised suspensions on peptide nanofibers. (A was adapted from *Science* 2001, **294**, 1684. Copyright © 2001 American Association for the Advancement of Science; B was adapted from *Nano Letters* 2007, **7**, 1165. Copyright © 2007 American Chemical Society; C was adapted from *Biomaterials* 2008, **29**, 161. Copyright © 2008 Elsevier Ltd; D was adapted from *J. Am. Chem. Soc.* 2004, **125**, 12756. Copyright © 2004 American Chemical Society.)

calcinations.⁵⁶ Recently, the simultaneous self-assembly, alignment, and patterning of peptide amphiphile nanofibers into well ordered nano-grooves has also been achieved using soft lithography (Fig. 10B).⁵⁵

4.6 Stabilisation of membrane proteins

Membrane proteins are important natural molecular devices in living cells and involved in many life functionalities such as

energy conversions, cell-cell communications and ion transport. They also work as natural biosensors for sight, hearing, smell, taste, touch and temperature.^{119–121} Therefore, they are particularly useful in current nanobiotechnology endeavour. However, there is a significant lack of understanding of their structures and functions due to the difficulties in extracting, purifying and stabilizing them.¹²² Simple but improved methods that can obtain membrane proteins without

disturbing their structures and biological functions have great potential in nanobiodevice fabrication.

Peptide amphiphiles have been reported as excellent materials to solubilise and stabilise membrane proteins (Fig. 11).^{31,32,34,95,122,123} Peptides V₆D, A₆D A₆K and V₆K can significantly increase the activity and stabilise diverse membrane proteins including *E. coli* glycerol-3-phosphate dehydrogenase,¹²³ G-protein coupled receptor-bovine rhodopsin⁷ and multi-domain protein complex photosystem-I (PS-I) on both dry surface³² and in aqueous solution.³⁴ They have been proven better than the commonly used membrane protein-stabilising detergents such as *N*-dodecyl- β -maltoside and *N*-octyl- β -glucoside.³² In addition, peptide A₆K can

stabilise the PS-I complex in a dried form at room temperature for at least 3 weeks. Both the polarity, the number of charges on the head group and the size and hydrophobicity of the tails have important effects on different membrane proteins.²

Apart from peptide amphiphiles, other peptides or lipopeptides have also been considered as excellent stabilisers for membrane proteins.¹²² Natural lipid bilayers provide not only the surrounding interactions but also suitable pressure to membrane proteins to retain their structures. Many membrane proteins lose their native structures and biological functions during the purification in the surfactant-solubilised state. Lipopeptides have very similar properties to membrane lipids and can provide suitable environment for membrane proteins. The lipopeptide used by McGregor *et al.*⁷⁰ has an α -helix structure. The polar residues are restricted to one side of the helix while the non-polar alanine residues are on the opposite site. Two acyl chains are attached at the two ends of the α -helix and interact with the non-polar alanine residues forming a surfactant feature (Fig. 11B). The length of the helical structure is similar to the width of a biological membrane. The lipopeptide has the capability to disrupt phospholipid bilayers and has proven to be effective at solubilising helical membrane proteins including bacteriorhodopsin and lactose (*lac*) permease, as well as the *E-coli* PagP protein.⁷⁰ Experimental studies aiming at elucidating the location and extent of peptide binding in the future will certainly expedite this area of research, leading to the design of more efficient peptides for protein stabilisation.

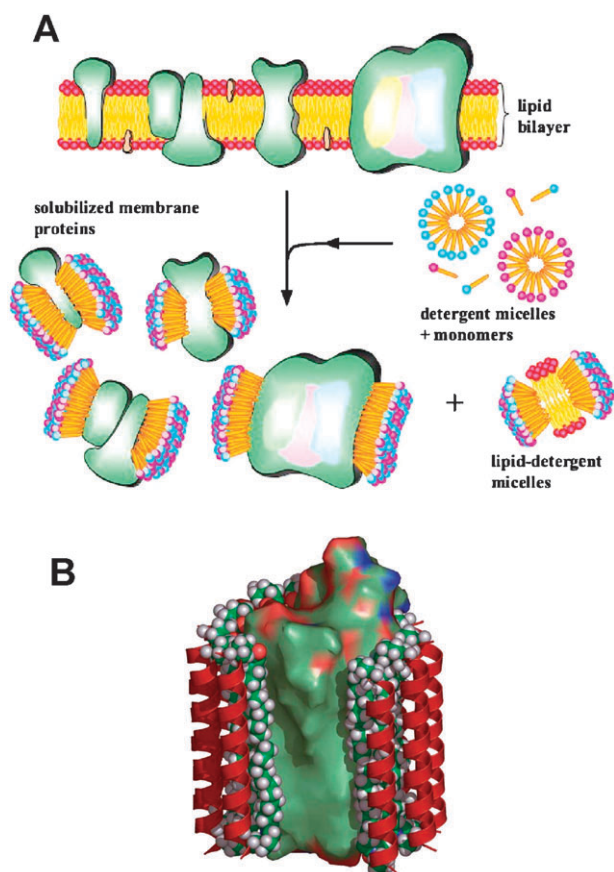


Fig. 11 A, a proposed scheme to illustrate how the designer peptide amphiphiles stabilise membrane proteins. Peptide amphiphiles have been used to solubilise, stabilise and crystallise membrane proteins. They use their tails to sequester the hydrophobic part of membrane proteins, with their hydrophilic heads exposed to water. Thus, their binding and association make membrane proteins soluble and stable outside the native cellular lipid milieu. These peptides are very important for overcoming the barrier of high-resolution molecular structures for challenging membrane proteins. B, representation of a proposed protein-lipopeptide complex. A solubilised membrane protein is represented by the solid surface. The peptide backbone of LPD-14 is represented by red ribbons, and the ornithines and alkyl chains are shown as space-filling spheres. The front most LPD monomers are omitted for clarity. (A was reproduced from *Chemical Society Reviews* 2006, **35**, 1105. Copyright © 2006 The Royal Society of Chemistry; B was reproduced from *Nature Biotechnology* 2003, **21**, 171. Copyright © 2003 Nature Publishing Group).

5. Conclusion remarks

Structural design and self-assembly of peptide amphiphiles have attracted increasing attention for both research and applications over the last decade, with an accelerated output over the past five years. This review only highlights representative studies of self-assembly of short peptides or lipopeptide amphiphiles that have displayed a wide range of interesting nanostructures. The studies have so far shown important effects of peptide chain length, the size of hydrophobic amino acid and the number of charge groups in the head on the size and shape of nanostructures. Other factors such as solution pH and ionic strength can also affect nanostructuring and hierarchical organisation. Examples of their applications in several important fields have been given where peptides and their self-assembled nanostructures work as reagents for killing bacteria, yeast and fungi, scaffolds for cell culture and tissue engineering, vectors and vehicles for drug and gene delivery, templates for nanofabrication and biomineralization and membrane protein stabilizers. Short peptide amphiphiles have also shown many other exciting and promising prospects which have not been covered in this review, for examples, in cell-free biology to enhance metabolic and synthetic activity and in surgery as biocompatible and biodegradable adhesives for stopping bleed and healing injury sites. Thus these peptide systems not only help us to tackle intractable biological phenomena such as protein folding and membrane protein studies, but they also play increasingly important roles in nanobiotechnology and nanomedicine. With better

understanding in structural design and self-assembly, future studies will focus more on exploiting new and improved applications.

Acknowledgements

The authors wish to thank the Engineering and Physical Sciences Research Council (EPSRC), Biotechnology and Biological Sciences Research Council (BBSRC) for funding support, the Royal Society for a UK-China Fellowship. We also thank the funding support from the Chinese National Key Lab of Heavy Oil Processing and National Natural Science Foundation of China (Grant Number 20773164). CH is supported by the Institute of Bioengineering and Nanotechnology (Biomedical Research Council, Agency for Science, Technology and Research, Singapore). SZ gratefully acknowledges support of a National Science Foundation grant CCR-0122419 to the MIT Center for Bits and Atoms, NIH BRP Grant EB003805 to CBE, ROHM Ltd., and generous gifts from Menicon Co. Ltd, Mitsui Chemicals, Inc., Mitsubishi Chemicals Corp., Intel Corp. SZ also gratefully acknowledges a fellowship from the John Simon Guggenheim Foundation.

References

- 1 S. Zhang, *Nat. Biotechnol.*, 2003, **21**, 1171.
- 2 Y. Yang, U. Khoe, X. Wang, H. Akihiro, H. Yokoi and S. Zhang, *Nano Today*, 2009, **4**, 193.
- 3 R. V. Ulijn and A. M. Smith, *Chem. Soc. Rev.*, 2008, **37**, 664.
- 4 E. H. C. Bromley, K. Channon, E. Moutevelis and D. N. Woolfson, *ACS Chem. Biol.*, 2008, **3**, 38.
- 5 M. E. Davis, P. C. H. Hsieh, T. Takahashi, Q. Song, S. Zhang, R. D. Kamm, A. J. Grodzinsky, P. Anversa and R. T. Lee, *Proc. Natl. Acad. Sci. U. S. A.*, 2006, **103**, 8155.
- 6 X. Yan, Q. He, K. Wang, L. Duan, Y. Cui and J. Li, *Angew. Chem., Int. Ed.*, 2007, **46**, 2431.
- 7 X. Zhao, Y. Nagai, P. J. Reeves, P. Kiley, H. G. Khorana and S. Zhang, *Proc. Natl. Acad. Sci. U. S. A.*, 2006, **103**, 17707.
- 8 F. Gelain, D. Bottai, A. Vescovi and S. Zhang, *PLoS One*, 2006, **1**, e119.
- 9 S. Zhang, *Nat. Biotechnol.*, 2004, **22**, 151.
- 10 V. Jayawarna, A. Smith, J. E. Gough and R. V. Ulijn, *Biochem. Soc. Trans.*, 2007, **35**, 535.
- 11 M. Zhou, A. M. Smith, A. K. Das, N. W. Hodson, R. F. Collins, R. V. Ulijn and J. E. Gough, *Biomaterials*, 2009, **30**, 2523.
- 12 V. Jayawarna, M. Ali, T. A. Jowitz, A. F. Miller, A. Saiani, J. E. Gough and R. V. Ulijn, *Adv. Mater.*, 2006, **18**, 611.
- 13 S. Zhang, F. Gelain and X. Zhao, *Semin. Cancer Biol.*, 2005, **15**, 413.
- 14 S. Zhang, L. Yan, M. Altman, M. L. Ssle, H. Nugent, F. Frankel, D. A. Laulenburg, G. M. Whitesides and A. Rich, *Biomaterials*, 1999, **20**, 1213.
- 15 C. E. Semino, J. Kasahara, Y. Hayashi and S. Zhang, *Tissue Eng.*, 2004, **10**, 643.
- 16 R. G. Ellis-Behnke, Y.-X. Liang, S.-W. You, D. K. C. Tay, S. Zhang, K.-F. So and a. G. E. Schneider, *Proc. Natl. Acad. Sci. U. S. A.*, 2006, **103**, 5054.
- 17 E. F. Banwell, E. S. Abelardo, D. J. Adams, M. A. Birchall, A. Corrigan, A. M. Donald, M. Kirkland, L. C. Serpell, M. F. Butler and D. N. Woolfson, *Nat. Mater.*, 2009, **8**, 596.
- 18 E. Kokkoli, A. Mardilovich, A. Wedekind, E. L. Rexeisen, A. Garga and J. A. Craig, *Soft Matter*, 2006, **2**, 1015.
- 19 R. N. Mitra, A. Shome, P. Paul and P. K. Das, *Org. Biomol. Chem.*, 2009, **7**, 94.
- 20 C. X. Chen, F. Pan, S. Z. Zhang, J. Hu, M. W. Cao, J. Wang, H. Xu, X. B. Zhao and J. R. Lu, *Biomacromolecules*, 2010, **11**, 402.
- 21 S. Zhang, *Materialstoday*, 2003, **6**, 20.
- 22 X. Zhao and S. Zhang, *Chem. Soc. Rev.*, 2006, **35**, 1105.
- 23 J. R. Lu, X. B. Zhao and M. Yaseen, *Curr. Opin. Colloid Interface Sci.*, 2007, **12**, 60.
- 24 R. J. Mart, R. D. Osborne, M. M. Stevens and R. V. Ulijn, *Soft Matter*, 2006, **2**, 822.
- 25 S. Zhang, *Biotechnol. Adv.*, 2002, **20**, 321.
- 26 S. Zhang, D. M. Marini, W. Hwang and S. Santoso, *Curr. Opin. Chem. Biol.*, 2002, **6**, 865.
- 27 X. Zhao and S. Zhang, *Macromol. Biosci.*, 2007, **7**, 13.
- 28 D. T. Bong, T. D. Clark, J. R. Granja and M. R. Ghadiri, *Angew. Chem., Int. Ed.*, 2001, **40**, 988.
- 29 A. Carlsen and S. Lecommandoux, *Curr. Opin. Colloid Interface Sci.*, 2009, **14**, 329.
- 30 H. Xu, J. Wang, S. Han, J. Wang, D. Yu, H. Zhang, D. Xia, X. Zhao, T. A. Waigh and J. R. Lu, *Langmuir*, 2009, **25**, 4115.
- 31 R. Das, P. J. Kiley, M. Segal, J. Norville, A. A. Yu, L. Wang, S. A. Trammell, L. E. Reddick, R. Kumar, F. Stellacci, N. Lebedev, J. Schnur, B. D. Bruce, S. Zhang and M. Baldo, *Nano Lett.*, 2004, **4**, 1079.
- 32 P. Kiley, X. Zhao, M. Vaughn, M. A. Baldo, B. D. Bruce and S. Zhang, *PLoS Biol.*, 2005, **3**, 1180.
- 33 U. Khoe, Y. Yang and S. Zhang, *Macromol. Biosci.*, 2008, **8**, 1060.
- 34 K. Matsumoto, M. Vaughn, B. D. Bruce, S. Koutsopoulos and S. Zhang, *J. Phys. Chem. B*, 2009, **113**, 75.
- 35 G. von-Maltzahn, S. Vauthey, S. Santoso and S. Zhang, *Langmuir*, 2003, **19**, 4332.
- 36 A. Nagai, Y. Nagai, H. Qu and S. Zhang, *J. Nanosci. Nanotechnol.*, 2007, **7**, 2246.
- 37 A. Yagmur, P. Laggner, S. Zhang and M. Rappolt, *PLoS One*, 2007, **2**, e479.
- 38 F. Pan, X. Zhao, S. Perumal, T. A. Waigh, J. R. Lu and J. R. P. Webster, *Langmuir*, 2010, **26**, 5690.
- 39 S. Santoso, W. Hwang, H. Hartman and S. Zhang, *Nano Lett.*, 2002, **2**, 687.
- 40 S. Vauthey, S. Santoso, H. Gong, N. Watson and S. Zhang, *Proc. Natl. Acad. Sci. U. S. A.*, 2002, **99**, 5355.
- 41 S. J. Yang and S. Zhang, *Supramol. Chem.*, 2006, **18**, 389.
- 42 U. Khoe, Y. Yang and S. Zhang, *Langmuir*, 2009, **25**, 4111.
- 43 H. Xu, Y. Wang, X. Ge, S. Han, S. Wang, P. Zhou, H. Shan, X. Zhao and J. R. Lu, *J. Am. Chem. Soc.*, submitted.
- 44 V. Breedveld, A. P. Nowak, J. Sato, T. J. Deming and D. J. Pine, *Macromolecules*, 2004, **37**, 3943.
- 45 T. J. Deming, *Soft Matter*, 2005, **1**, 28.
- 46 J. A. Hanson, C. B. Chang, S. M. Graves, Z. Li, T. G. Mason and T. J. Deming, *Nature*, 2008, **455**, 85.
- 47 W. Y. Seow and Y.-Y. Yang, *Adv. Mater.*, 2009, **21**, 86.
- 48 X. D. Guo, F. Tandiono, N. Wiradharma, D. Khor, C. G. Tan, M. Khan, Y. Qian and Y.-Y. Yang, *Biomaterials*, 2008, **29**, 4838.
- 49 N. Wiradharma, Y. W. Tong and Y.-Y. Yang, *Biomaterials*, 2009, **30**, 3100.
- 50 N. Wiradharma, M. Khan, Y. W. Tong, S. Wang and Y.-Y. Yang, *Adv. Funct. Mater.*, 2008, **18**, 943.
- 51 A. J. van-Hell, C. I. C. A. Costa, F. M. Flesch, M. Sutter, W. Jiskoot, D. J. A. Crommelin, W. E. Hennink and E. Mastrobattista, *Biomacromolecules*, 2007, **8**, 2753.
- 52 M. Deng, D. Yu, Y. Hou and Y. Wang, *J. Phys. Chem. B*, 2009, **113**, 8539.
- 53 J. D. Hartgerink, E. Beniash and S. I. Stupp, *Proc. Natl. Acad. Sci. U. S. A.*, 2002, **99**, 5133.
- 54 J. D. Hartgerink, E. Beniash and S. I. Stupp, *Science*, 2001, **294**, 1684.
- 55 A. M. Hung and S. I. Stupp, *Nano Lett.*, 2007, **7**, 1165.
- 56 V. M. Yuwono and J. D. Hartgerink, *Langmuir*, 2007, **23**, 5033.
- 57 T. Shimada, S. Lee, F. S. Bates, A. Hotta and M. Tirrell, *J. Phys. Chem. B*, 2009, **113**, 13711.
- 58 H. Cui, T. Muraoka, A. G. Cheetham and S. I. Stupp, *Nano Lett.*, 2009, **9**, 945.
- 59 M. A. Greenfield, J. R. Hoffman, M. O. d. l. Cruz and S. I. Stupp, *Langmuir*, 2010, **26**, 3641.
- 60 M. J. Webber, J. Tongers, M.-A. Renault, J. G. Roncalli, D. W. Losordo and S. I. Stupp, *Acta Biomater.*, 2010, **6**, 3.
- 61 D. A. Harrington, E. Y. Cheng, M. O. Guler, L. K. Lee, J. L. Donovan, R. C. Claussen and S. I. Stupp, *J. Biomed. Mater. Res., Part A*, 2006, **78a**, 157.

- 62 A. Makovitzki, J. Baram and Y. Shai, *Biochemistry*, 2008, **47**, 10630.
- 63 D. Missirlis, H. Khant and M. Tirrell, *Biochemistry*, 2009, **48**, 3304.
- 64 H.-w. Jun, S. E. Paramonov, H. Dong, N. Forraz, C. McGuckin and J. D. Hartgerink, *J. Biomater. Sci., Polym. Ed.*, 2008, **19**, 665.
- 65 J.-K. Kim, J. Anderson, H.-W. Jun, M. A. Repka and S. Jo, *Mol. Pharmaceutics*, 2009, **6**, 978.
- 66 L. Liu, K. Xu, Huaying Wang, J. T. P. K., W. Fan, S. S. Venkatraman, L. Li and Y.-Y. Yang, *Nat. Nanotechnol.*, 2009, **4**, 457.
- 67 A. Mata, L. Hsu, R. Capito, C. Aparicio, K. Henrikson and S. I. Stupp, *Soft Matter*, 2009, **5**, 1228.
- 68 L. R. Robinson, N. C. Fitzgerald, D. G. Doughty, N. C. Dawes, C. A. Berge and D. L. Bissett, *Int. J. Cosmet. Sci.*, 2005, **27**, 155.
- 69 R.-I. Chirita, P. Chambault, J.-C. Archambault, I. Robert and C. Elfakir, *Anal. Chim. Acta*, 2009, **641**, 95.
- 70 C.-L. McGregor, L. Chen, N. C. Pomroy, P. Hwang, S. Go, A. Chakrabarty and G. G. Privé, *Nat. Biotechnol.*, 2003, **21**, 171.
- 71 X. Zhao, F. Pan and J. R. Lu, *Prog. Nat. Sci.*, 2008, **18**, 653.
- 72 L. Stryer, *Biochemistry*, W.H. Freeman and Company, 1988.
- 73 S. E. Paramonov, H.-W. Jun and J. D. Hartgerink, *J. Am. Chem. Soc.*, 2006, **128**, 7291.
- 74 D. Ranganathan, C. Lakshmi and I. L. Karle, *J. Am. Chem. Soc.*, 1999, **121**, 6103.
- 75 D. Haldar, S. K. Maji, M. G. B. Drew, A. Banerjee and A. Banerjee, *Tetrahedron Lett.*, 2002, **43**, 5465.
- 76 M. R. Ghadiri, J. R. Granja, R. A. Milligan, D. E. McRee and N. Khazanovich, *Nature*, 1993, **366**, 324.
- 77 J. D. Hartgerink, J. R. Granja, R. A. Milligan and M. R. Ghadiri, *J. Am. Chem. Soc.*, 1996, **118**, 43.
- 78 H. Yang, S.-Y. Fung, M. Pritzker and P. Chen, *PLoS One*, 2007, **2**, e1325.
- 79 B. G. Cousins, A. K. Das, R. Sharma, Y. Li, J. P. McNamara, I. H. Hillier, I. A. Kinloch and R. V. Ulijn, *Small*, 2009, **5**, 587.
- 80 A. K. Das, R. Collins and R. V. Ulijn, *Small*, 2008, **4**, 279.
- 81 S. Toledano, R. J. Williams, V. Jayawarna and R. V. Ulijn, *J. Am. Chem. Soc.*, 2006, **128**, 1070.
- 82 A. Laromaine, L. Koh, M. Murugesan, R. V. Ulijn and M. M. Stevens, *J. Am. Chem. Soc.*, 2007, **129**, 4156.
- 83 J. C. Stendahl, M. S. Rao, M. O. Guler and S. I. Stupp, *Adv. Funct. Mater.*, 2006, **16**, 499.
- 84 J. P. Schneider, D. J. Pochan, B. Ozbas, K. Rajagopal, L. Pakstis and J. Kretsinger, *J. Am. Chem. Soc.*, 2002, **124**, 15030.
- 85 D. A. Salick, J. K. Kretsinger, D. J. Pochan and J. P. Schneider, *J. Am. Chem. Soc.*, 2007, **129**, 14793.
- 86 M. S. Lamm, N. Sharma, K. Rajagopal, F. L. Beyer, J. P. Schneider and D. J. Pochan, *Adv. Mater.*, 2008, **20**, 447.
- 87 L. A. Haines-Butterick, D. A. Salick, D. J. Pochan and J. P. Schneider, *Biomaterials*, 2008, **29**, 4164.
- 88 M. C. Branco, D. J. Pochan, N. J. Wagner and J. P. Schneider, *Biomaterials*, 2009, **30**, 1339.
- 89 R. P. Nagarkar, Rohan A. Hule, D. J. Pochan and J. P. Schneider, *J. Am. Chem. Soc.*, 2008, **130**, 4466.
- 90 R. A. Hule, Radhika P. Nagarkar, A. Altunbas, H. R. Ramay, M. C. Branco, J. P. Schneider and D. J. Pochan, *Faraday Discuss.*, 2008, **139**, 251.
- 91 T. Yucel, C. M. Micklitsch, J. P. Schneider and D. J. Pochan, *Macromolecules*, 2008, **41**, 5763.
- 92 L. Haines-Butterick, K. Rajagopal, M. Branco, D. Salick, R. Rughani, M. Pilarz, M. S. Lamm, D. J. Pochan and J. P. Schneider, *Proc. Natl. Acad. Sci. U. S. A.*, 2007, **104**, 7791.
- 93 M. C. Branco and J. P. Schneider, *Acta Biomater.*, 2009, **5**, 817.
- 94 R. V. Rughani and J. P. Schneider, *MRS Bulletin*, 2008, **33**, 530.
- 95 W. S. Childers, R. Ni, A. K. Mehta and D. G. Lynn, *Curr. Opin. Chem. Biol.*, 2009, **13**, 652.
- 96 X. Zhao, F. Pan, S. Perumal, H. Xu, J. R. Lu and J. R. P. Webster, *Soft Matter*, 2009, **5**, 1630.
- 97 M. O. Guler, L. Hsu, S. Soukasene, D. A. Harrington, J. F. Hulvat and S. I. Stupp, *Biomacromolecules*, 2006, **7**, 1855.
- 98 M. O. Guler, S. Soukasene, J. F. Hulvat and S. I. Stupp, *Nano Lett.*, 2005, **5**, 249.
- 99 M. K. Baumann, M. Textor and E. Reimhult, *Langmuir*, 2008, **24**, 7645.
- 100 S. Bucak, C. Cenker, I. Nasir, U. Olsson and M. Zackrisson, *Langmuir*, 2009, **25**, 4262.
- 101 X. Zhao, F. Pan and J. R. Lu, *J. R. Soc. Interface*, 2009, **6**, S659.
- 102 J. Wang, S. Han, G. Meng, H. Xu, D. Xia, X. Zhao, R. Schweins and J. R. Lu, *Soft Matter*, 2009, **5**, 3870.
- 103 A. P. Nowak, V. Breedveld, L. Pakstis, B. Ozbas, D. J. Pine, D. Pochan and T. J. Deming, *Nature*, 2002, **417**, 424.
- 104 H. Heerklotz and J. Seelig, *Biophys. J.*, 2001, **81**, 1547.
- 105 H.-K. Lee, S. Soukasene, H. Jiang, S. Zhang, W. Feng and S. I. Stupp, *Soft Matter*, 2008, **4**, 962.
- 106 T. Muraoka, H. Cui and S. I. Stupp, *J. Am. Chem. Soc.*, 2008, **130**, 2946.
- 107 T. Muraoka, C.-Y. Koh, H. Cui and S. I. Stupp, *Angew. Chem., Int. Ed.*, 2009, **48**, 5946.
- 108 K. L. Niece, C. Czeisler, V. Sahni, V. Tysseling-Mattiace, E. T. Pashuck, J. A. Kessler and S. I. Stupp, *Biomaterials*, 2008, **29**, 4501.
- 109 K. A. Brogden, *Nat. Rev. Microbiol.*, 2005, **3**, 238.
- 110 M. Zasloff, *Nature*, 2002, **415**, 389.
- 111 A. Giuliani, G. Pirri, A. Bozzi, A. D. Giulio, M. Aschi and A. C. Rinaldi, *Cell. Mol. Life Sci.*, 2008, **65**, 2450.
- 112 S. Ghanaati, M. J. Webber, R. E. Unger, C. Orth, J. F. Hulvat, S. E. Kiehna, M. Barbeck, A. Rasic, S. I. Stupp and C. J. Kirkpatrick, *Biomaterials*, 2009, **30**, 6202.
- 113 M. Kanlayavattanakul and N. Lourith, *Int. J. Cosmet. Sci.*, 2010, **32**, 1.
- 114 M. B. Dickerson, K. H. Sandhage and R. R. Naik, *Chem. Rev.*, 2008, **108**, 4935.
- 115 H. Jiang, M. O. Guler and S. I. Stupp, *Soft Matter*, 2007, **3**, 454.
- 116 T. D. Sargeant, M. O. Guler, S. M. Oppenheimer, A. Mata, R. L. Satcher, D. C. Dunand and S. I. Stupp, *Biomaterials*, 2008, **29**, 161.
- 117 E. D. Spoerke, S. G. Anthony and S. I. Stupp, *Adv. Mater.*, 2009, **21**, 425.
- 118 E. D. Sone and S. I. Stupp, *J. Am. Chem. Soc.*, 2004, **126**, 12756.
- 119 E. Wallin and G. Von-Heijne, *Protein Science*, 1998, **7**, 1029.
- 120 P. J. Loll, *J. Struct. Biol.*, 2003, **142**, 144.
- 121 J. Nilsson, B. Persson and G. von-Heijne, *Proteins: Struct., Funct., Bioinf.*, 2005, **60**, 606.
- 122 G. G. Privé, *Curr. Opin. Struct. Biol.*, 2009, **19**, 379.
- 123 J. I. Yeh, S. Du, A. Tortajada, J. Paulo and S. Zhang, *Biochemistry*, 2005, **44**, 16912.